Feasibility Study on Concrete Sandwich Panels As Innovative Building Systems for Residential Construction

FINAL YEAR PROJECT UG 2017

By

Umair Abid Mughal	00000 212593
Muhammad Nouman Anwar	00000 211303
Muhammad Uzair Khan	00000 210065
Faizan Masood	00000 209755

NUST Institute of Civil Engineering (NICE)

School of Civil and Environmental Engineering (SCEE)

National University of Science and Technology (NUST), Islamabad, Pakistan

2021

This is to certify that the Final Year Project Titled

"Feasibility Study on Concrete Sandwich Panels as Innovative Building Systems for Residential Construction"

Submitted By

Umair Abid Mughal	00000 212593
Muhammad Nouman Anwar	00000 211303
Muhammad Uzair Khan	00000 210065
Faizan Masood	00000 209755

has been accepted towards the requirements for the undergraduate degree

in

CIVIL ENGINEERING

_____

Dr. Rao Arsalan Khushnood
Associate Professor
NUST Institute of Civil Engineering
School of Civil and Environmental Engineering
National University of Sciences and Technology, Islamabad, Pakistan

DEDICATION

To our beloved parents, teachers, mentors and colleagues who have stood by our side in rough and tough times, who have taught us to show perseverance in the face of adversity.

ACKNOWLEDGEMENTS

In the name of Allah, the most Beneficent, the most Merciful as well as peace and blessings upon Prophet Muhammad, His servant and final messenger.

First of all, we would like to thank our Creator Allah the Almighty, who has blessed us with the opportunity to perform this research. His guidance through each and every adversity while carrying out our research work, is what has led us to complete and compile our work in time.

We are also greatly thankful to our parents who have supported us through every thick and thin of our life's journey. They have supported us when we were not able to walk, and they are still supporting us to continue and provide solutions for humanity.

We are also obliged from the depths of our hearts to pay special thanks to our supervisor, Dr. Rao Arsalan Khushnood. His guidance throughout the project has been a great learning experience for us and the knowledge he has imparted in us will be one the primary factors for our growth. He has also helped us in every part of our thesis and above all, his constant efforts to expose our project on a bigger stage will be a key factor to help us dive into the practical world. We feel the responsibility to thank him for his patience, guidance, and cooperation throughout our final year project.

We are also extremely grateful to and value the assistance provided by Mr. Matiullah Shah and the entire staff of Structures Lab at NICE. They have been a vital element to our success and have helped us conduct experiments and procure materials and equipment, despite the restrictions and harsh conditions brought about by COVID-19

Finally, I, Umair Abid, the group leader for this project, would like to pay my sincerest gratitude to my dear group members, who took matters into hand, followed my guidance by heart, sacrificed their sleep and carried out experimental work in scorching heat despite fasting, when time of adversity came upon me. Lastly, we as a group, would like to pay our gratitude to anyone and everyone, who participated knowing and unknowingly, to assist us in our endeavors while carrying out this study.

ABSTRACT

The aim of this project was to research and devise a structural configuration of lightweight sandwich panels, which would offer a solution for rapid and economical residential construction in Pakistan. The first phase of the project aimed at optimizing a suitable material configuration for mortar-wythes by integration of Fly Ash (Class-C) and Waste Marble Powder (WMP), which are potential indigenous wastes, to promote sustainability. Three mix recipes consisting of fly ash and waste marble powder replaced at 15% by weight of cement and control mix-recipe were tested for compressive strength, flexural strength, carbonation, chloride-ion penetration, drying shrinkage and flow-ability. The results revealed that all the mix recipes yielded a compressive strength in excess of 25 MPa and flexural strength in excess of 10 MPa, in addition to satisfying the criteria for carbonation, chloride ion penetrability, drying shrinkage and flow-ability, making the optimized mixes suitable for structural layers in sandwich panels. The second phase of this project consisted of devising structural configuration for sandwich panels, fabricating the finalized panel configuration and testing the scaled samples of panels in compression and flexure. Sandwich panels comprising of 50 mm mortar wythes and 80 mm EPS insulation layer with steel connectors spaced at 150 mm were chosen to be the proposed configuration. Four scaled sandwich panels with dimensions 750mm x 300mm x 186mm were fabricated and tested in compression. Moreover, one scaled panel with dimensions 1500mm x 1200mm x 186mm was casted, cured and tested in flexure using three-point bending test. The compression test results revealed sandwich panels were able to withstand compressive forces in excess of 600 kN, whereas the load at first crack during flexure testing was found out to be 32.5 kN. In addition, the thermal transmittance value of the scaled panel was evaluated using Heat flow apparatus and the average thermal transmittance (U-value) was found out to be 0.385 $W/m^2.k$. The results of thermal conductivity test were used to conduct thermal analysis of the proposed panels using ECOTECT software and results revealed over 47.5% reduction in cooling loads, electricity costs, and CO_2 emissions during life-cycle of building and over 12 times reduction in CO_2 emissions during manufacturing phase when compared to manufacturing of burnt bricks

TABLE OF CONTENTS

LIST OF FIGURES

LIST OF TABLES

CHAPTER 1: INTRODUCTION

1.1 General

For the development of third-world countries, affordable quality housing with rapid construction potential is crucial. Conventional construction systems and techniques like brick masonry construction and R.C.C construction might offer many benefits at hindsight such as economy in material and labor, non-skilled labor, widely available construction materials, low-cost construction etc. but their drawbacks such as limited building spans and heights, excessive labor, thick structural elements, energy inefficiency and large construction times indicate that conventional construction technologies aren't the best solution for affordable and rapid quality housing. Their benefits may make them economical in the short-term, but when evaluated for the long-term, their operational costs add up and hence, these systems don't provide a viable solution.

For a developing country like Pakistan, these conventional construction techniques don't offer a viable solution to meet the needs of affordable, low maintenance and quality housing. In addition, burnt bricks and cement production in Pakistan are becoming a major reason for the rising CO2 emissions and rising global warming levels. Moreover, with many new initiatives like the Naya Pakistan Housing Program (NPHP), whose primary aim is to solve the problem of housing shortage in Pakistan and provide affordable quality housing for all, a new form of housing technology needs to be relied on. The Naya Pakistan Housing Program is set to give the rural people of Pakistan a life of contentment and ease by constructing 5 million affordable/low-cost houses [1]

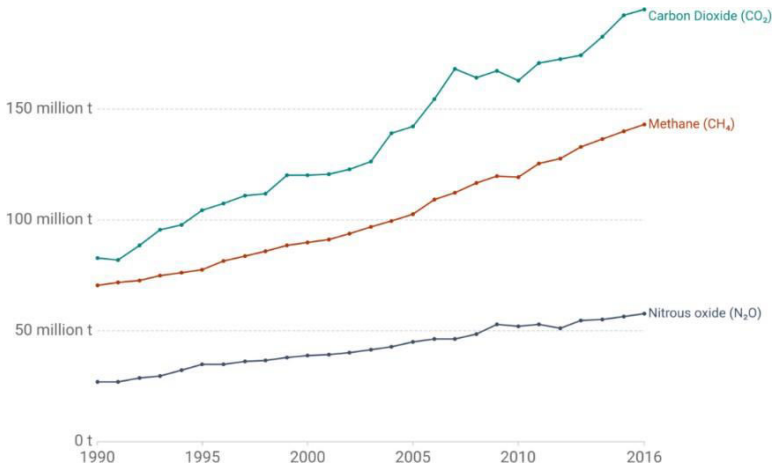

Figure. 1.1.1: *Greenhouse gas emissions by gas source, measured in tones of CO2 equivalents, Pakistan (Source: CAIT Climate Data Explorer via. Climate Watch)*

1.2 Concrete Sandwich Panels

Pre-cast Concrete Sandwich Panels (PCSP) are innovative building systems which consist of a rigid insulation layer such as expanded polystyrene (EPS), which is sandwiched or embedded between two layers of structural or non-structural concrete wythes. These construction systems are used widely in residential and industrial building due to their low self-weight, thermal efficiency and high strength to weight ratios [17 – 19]. The role of the concrete layers is to provide the system with structural capacity needed to bear loads when used for structural applications, in addition to shielding the insulation layer from external deteriorating effects of weathering, harmful particles in the air and fire hazards.

Structural lightweight sandwich panels offer various benefits when compared to conventional construction technologies. These benefits include lightweight as compared to full concrete section, thermal efficiency provided because of thermal insulation and reduction in reliance of heavy equipment and machinery for the transportations and construction of structures on site when compared to regular pre-cast concrete sections [2,3]. In addition, pre-cast sandwich panels have been found out to be excellent flexural members when sufficient composite action is achieved between the various panel layers. Hence, pre-cast concrete sandwich panels can be used as slabs and have been found out to be excellent alternative to conventional concrete slab system in moderate sized structures [4]. Stability and increased out of plane bearing capacities can be achieved using a series of steel shear connectors between the different layers [18, 20]. A typical configuration of reinforcement and layers is shown in Figure 1.2.1 (a) and 1.2.1 (b)

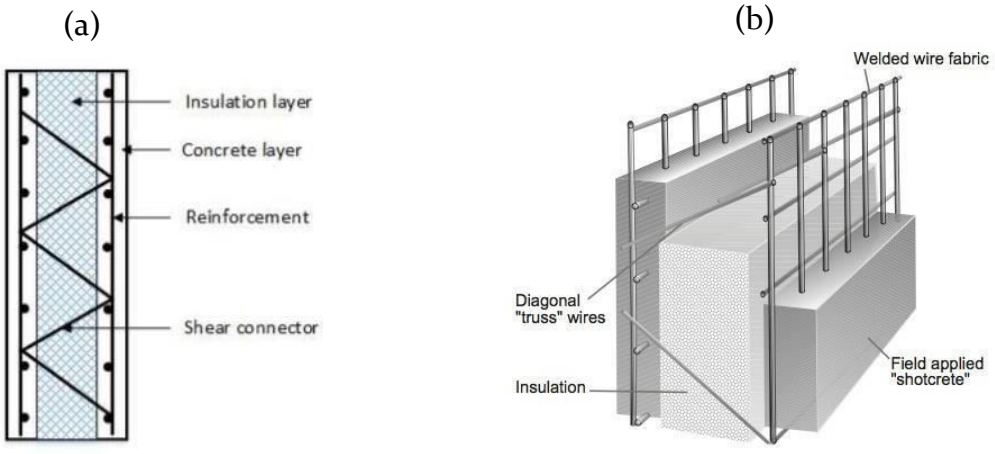

Figure 1.2.1 (a) and (b): *Components of a typical concrete sandwich panel [55]*

1.3 Shear Reinforcement

Reinforcement in the form of shear connectors is required for the concrete wythes to transfer shear force between them; hence, shear connectors determine the degree of composite action. An effective shear connector provides sufficient shear transfer between the concrete layers for full composite action [5]. Typically, a structural precast concrete sandwich panel is one which exhibits composite action due to reinforced concrete face wythes and adequate shear connectors.

Sandwich structures can be compared to I-beam, where the facings of the panel represent flanges of an I-beam since they're the structural components in the panels responsible for carrying the bending stress; and core, composed of insulation layer and shear connectors, corresponds to the web of the I-beam as it is primary responsible to resist the shear loads and stabilizes the faces against buckling action [6]. Therefore, the core must be rigid enough to ensure that the two concrete wythes remain separated by a proper distance and don't displace relative to each other and form a single stress profile across the cross-section of the whole panel [5, 7]. Hence, shear connectors, which induce rigidity into the core, are an integral part of the composite beam design.

In situations where the amount of shear connectors is not adequate to provide adequate shear strength between the two concrete wythes, either partially composite or non-composite action is achieved and the two concrete wythes would behave as two independent beams or panels, with separate stress profiles [4]. In a fully-composite or a partially-composite concrete panel, such as in panels reinforced with steel truss connectors, bent steel bar connectors and solid concrete zones, shear forces are transferred effectively, allowing the two concrete wythes to behave as a homogenous element, displace by the same amounts and resist loads together. Whereas, in panels with non-composite or non-shear connectors, such as metallic and fiber-reinforced connectors, shear force is transferred is in very small amount that it can be considered negligible; and hence, the two structural or non-structural concrete wythes behave as separate elements [4, 8]. Figure 1.3.1 (a), (b) and (c) show strain profiles in composite, partially composite and non-composite panels. Amran et al. tested lightweight sandwich panels in flexure and found out that the typical failure occurred when the tested specimens reached their ultimate load due to major cracks that extended significantly along the bottom concrete wythe, especially at the mid-span; a behavior exhibited in composite I-sections or beams [8]

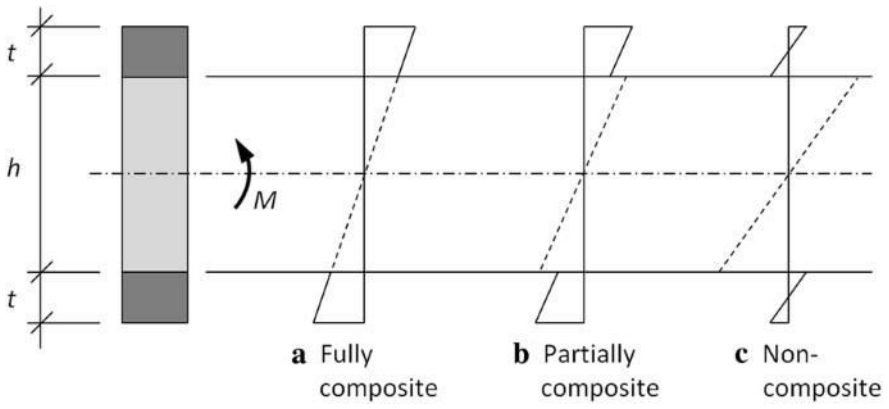

Figure 1.3.1: *Strain profiles in (a) composite, (b) partially composite and (c) non-compositepanel*

1.4 Autodesk® Ecotect® Analysis

Autodesk® Ecotect® Analysis is a comprehensive concept-to-detail energy simulation software that is compatible as an add-on tool with Building Information Modelling (BIM) software, such as Autodesk Revit and can be used to perform building energy performance analysis. Autodesk® Ecotect® Analysis offers a wide range of simulation and building energy analysis functionality that can improve performance of existing buildings and new building designs. It combines an interactive 3-dimentional interface with a wide list of performance analysis functions and intuitive information displays. The software runs a number of simulations to generate analytical results of the building's performance even before the building is constructed, by taking into account various parameters such as environmental factors, the thermal properties of building materials, the architectural layout and dimensions of the structure to be constructed etc. Ecotect provides acoustic, thermal and lighting analyses, including hourly thermal comfort, monthly space loads, natural and artificial lighting levels, acoustic reflections, reverberation time, project costs and environmental impact [74, 75]

Building Sector accounts for a great portion of the energy consumption and it is expected that this this value is only expected to increase from here on onwards as the livings standards, energy demands, urban population and building technologies change overtime. Similarly, in Pakistan, it has been stated that 50% of the total energy consumption is associated with the construction and building industry [86]. Moreover, global warming and climate change are two of the main reasons that energy demands are expected to increase within the coming years and with Pakistan being the 5th most

affected country due to adverse effects of global warming in 2020 [87], the need to come-up with sustainable and energy efficient housing is ever increasing.

Figure 1.4.1: *Time Series of Area-Weighted Mean Daily Temperatures Averages over Each Year from 1960 to 2013*

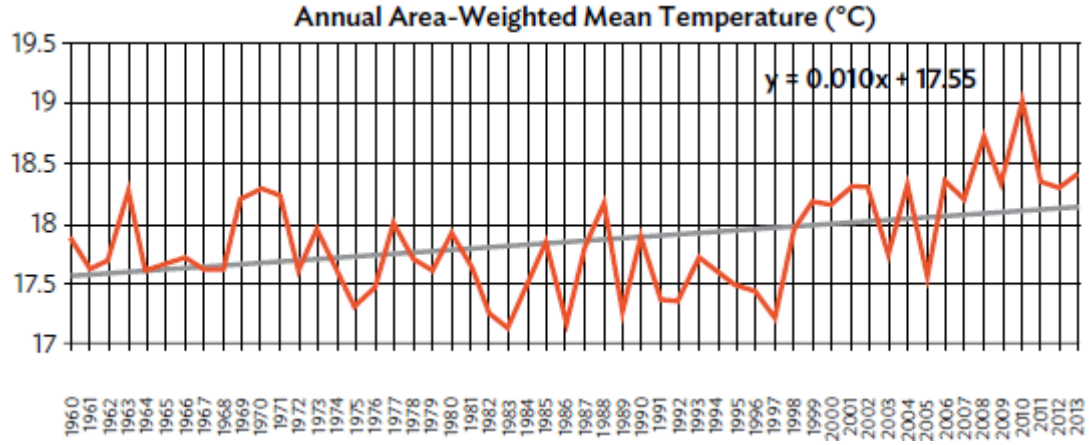

Notes: *Red line = Area-weighted mean temperature of Pakistan, Black line = Linear trend (rate of change = 0.01°C), Total Change = 0.54°C*

Source: Modified from G.Rasul et al. 2012b. Climate Change in Pakistan Focused on Sindh Province. Technical Report. No. 25. Islamabad: Pakistan Metrological Department

1.5 Objectives

The salient objectives of this research are to:

1) Devise a structural configuration for fabrication of light-weight sandwich panels offering solutions for rapid and economical residential construction in Pakistan
2) Optimize material configuration of mortar wythes by integration of potential indigenous wastes promoting sustainability
3) Investigate the adequacy of fabricated light-weight sandwich panels as structural walls and floor systems in residential structures
4) Present a methodology for estimating the CO_2 emissions generated over a building's life cycle and perform quantitative analysis on the carbon emissions by use of concrete sandwich panels.

CHAPTER 2: LITERATURE REVIEW

2.1 Shear Connectors

In past studies, different shapes of shear connectors and adhesive between the layers have been used to estimate the structural strength of panels. Wall panels with glass fiber reinforced polymer shear sheets, adhesive, and mechanical bonds between insulation and concrete wythe can be used [9, 10]. By using glass fiber reinforced polymer grid type shear connectors, it is possible to achieve a high degree of composite action and structural strength, as well as better thermal insulation properties due to reduction in thermal bridging effect, where heat transfer between wythes takes place via shear connectors. It was also determined that continuous type shear connectors provided for better performance when compared to stud type connectors [11,12]
Experimental programs verified that using lower mesh size does not drastically increase the panel's total flexural load carrying capacity as panels with rebars do [2,7]. Moreover, experimental data has also revealed that inclined shear connectors display better shear transfer when diameter of connector increases [13, 14]

Basalt fiber reinforcement was used as shear connectors and longitudinal reinforcement. Results showed that sufficient composite action and ultimate strengths were achieved attributing to the high elastic modulus of basalt fiber reinforcement and sufficient reduction in thermal bridging was achieved because of lesser thermal conductivity of basalt fiber when compared to steel reinforcement [15]

An experimental program was developed to test the ultimate strengths of panels with three different types of shear connector reinforcement: Steel, Carbon Fiber rods and Carbon Fiber Strips. Results showed the panel with carbon fiber strips showed the greatest ultimate strengths, followed by steel and then carbon fiber rods. Carbon fiber strips resulted in greater ultimate strengths due to wider area of cross-section when compared to carbon fiber rods. Degree of composite action was also determined for the three configurations and results revealed the greatest degree of composite action in panels using carbon fiber strips as shear connectors (89.29% Degree of composite action), followed by Steel shear connectors (85.11% Degree of composite action) and lastly carbon fiber rods (75.07% degree of composition action). Results of strength/weight ratio displayed the same patterns.

The experimental program also revealed that panels utilizing 45° shear connectors resulted in around 23% greater ultimate loads in flexure when compared to 60° shear connectors and around 33.3% greater ultimate loads when compared to panels using the same connectors at 90° [16]

2.2 Panels in Compression

As mentioned earlier, there are several papers that have focused on the behavior of panels in flexure [3-16] but few studies have been done to evaluate the behavior of panels in compression [21-26]. Similarly, fewer studies have focused on the factors which affect the compressive strength of panels such as thickness of layers, diameter or distribution of shear connectors [18]. Aguado et al. conducted an experimental study to determine the behavior of panels in compression by varying parameters such as thickness of layers, distance between shear connectors, positioning of steel mesh, and develop an analytical formulation to estimate the ultimate strength of panels [27]. Increasing the thickness of EPS core result in significant reduction in the ultimate compressive load of the panels. Compressive strength of the mortar caused a significant change in the ultimate load handled by the scaled panel specimen. Generally, a larger change was seen for panels with thinner EPS cores. Varying the aspect ratio of panels by increasing height of panel specimen resulted in considerable reduction in maximum loads due to bending moments caused by eccentric loading. Increasing the thickness of mortar wythes results in considerable increase in the maximum load taken [27]. The study also developed relationship between position of wire-mesh in the mortar wythes and determined center positioning to be most efficient based on theoretical analysis

2.3 Autodesk® Ecotect®

2.3.1 Thermal Comfort Analysis of Sandwich Panels

Cheung et al conducted thermal comfort analysis for high-rise building in hot and humid climate in 2005 and found out that electricity usage by cooling load can be reduced by up to 34.1% on annual basis and 36.8% on peak cooling loads by changing the building envelope of the structure by use of better and more efficient construction materials, insulation materials, thermal mass, lighter colored paints for external walls, using glazed windows and shading [88]. In addition to this, another research concluded that another way to conserve the overall energy of the house is by proper planning and

orientation of the house and through appropriate control of the air conditioning and heating [89]. Research by Arif, et. al. conducted at architectural department in Lahore saw cooling loads decrease by up to 29% when a simple EPS insulation layer was added to the existing architecture of the building [90]. In a similar research on a 205 ft² single-story building in DHA society in Karachi, Nafeesa, et. al., conducted a theoretical study using Autodesk® Ecotect® Analysis software, studying the effect of adding glazed windows, aerated concrete blocks and other insulating materials on the existing building and the resulting increase in thermal efficiency and found out energy savings of up to 35% in cooling loads and 82% in heating loads [71].

Past literature indicates that 50-70% of the heat transfer in single and double story buildings takes place via the roof and hollow clay blocks when used as insulation materials in roofs can improve the thermal efficiency of buildings by 40-63% when compared to conventional roof systems [91, 92]. As a contract, floors can also improve the thermal efficiency of buildings. Thermal mass, a material capable of absorbing, storing and releasing heat based on the surrounding temperatures can help reduce temperatures in hot climates whereas raise temperatures in cold climates [93]. In addition, raised floor slabs can also improve thermals of a building by providing cavities which acts as insulation media [94]. Similarly, past research has also highlighted the importance of walls as another building envelope component which can provide thermal and acoustic comfort [95]. Using wall insulations, heating and cooling demands of the structure can be significantly reduced [96]. Moreover, using light light-colored paints and reflective media on the external walls can also provide thermal comfort as indicated by past literature [97]. Lastly, increasing the wall thickness can bring about 7-10% savings in cooling loads as the width of barrier between external and internal environment is increased [98].

2.3.2 Life-cycle Carbon Emission

Past literature has indicated that Ecotect simulations provide reasonably good accuracy [76, 77, 78]. [79] conducted a Life cycle assessment (LCA) study on a commercial building using Ecotect software using a BIM model accurately representing the real-life structure. The scope of the study was to compare the distribution of various design parameters such as CO_2 emissions and energy consumption at various stages of the design life of the building. In addition, several parameters were varying to conduct a sensitivity analysis and identify the prime parameter which most impacted the

performance of the structure. The results indicated that several parameters affected the performance of building with varying degrees, rather than a single parameter overpowering the results.

[80] performed CO_2 emission analysis on a single-story building in Sweden and that 85% of the total embodied carbon energy use occurred during the operational phase, following by 15% embodied energy use during the manufacturing the construction materials and construction of the dwelling. Transportation and energy use during demolition accounted for only 1% of the total embodied energy during the life cycle of the structure and hence, these values can be ignored and still a performance analysis with responsible accuracy can be achieved. [81] deducted that structural and finishing materials directly and indirectly represent the largest relative contribution in embodied energy during life-cycle of building. The contributions of equipment, construction and transportation were insignificant in comparison to the construction and finishing materials.

[82, 83, 84] found out that embodied energy contributes to only a mere 10-20% of a structure's total carbon emission in life cycle; however, the potential to reduce its percentage should not be ignored. Embodied carbon emissions can characteristically be reduced by use of innovative building materials that reduce the use of carbon during manufacturing stage and make the building thermally efficient to reduce operational embodied carbon use [85]. Moreover, [86, 87] concluded that embodied carbon emission can be reduced by up to 30-45% in residential structures by use of new and innovative construction techniques and technologies and by use of low-carbon materials.

CHAPTER 3: EXPERIMENTAL PROGRAM, MATERIALS AND METHOLODY

3.1 Mix Formulation

For this research, a total of three mix formulations were prepared for the mortar wythes of the PCSP. These include one control mix which was prepared without the addition of any supplementary cementitious material (SCM) and two of the remaining mix formulations were prepared by incorporating Fly Ash (FA) as a partial replacement of cement by its weight at 15% and Waste Marble Powder (WMP) replaced at 15% by weight of cement. In addition, superplasticizer (SP) was also added by percentage of the weight of the binder to reduce the water/binder requirement and increase the strength of the mixture by maintaining a steady flow. The ratio of binder to sand was kept as 1: 3.1 in all of the mixes to target a 28-day compressive strength of 25 MPa. The optimum water/binder ratio (w/b) and the percentage of superplasticizer (SP) were adjusted by trial and error after a steady flow of 210±10 mm was achieved in flow table apparatus as required by ASTM C270 [33]. The details of the formulations are shown in Table 3.1.1**.** The typical formulations in Table 3.1.2 such as C85-FA can be read as 85% cement, 15% FA, w/b = 45% and SP = 1% of cement

Table 3.1.1: *Details of mix formulations for Mortar Wythes*

Serial	Formulation	Cement (%)	Fly Ash (%)	Waste Marble Powder (%)
1.	C100	100	0	0
2.	C85-FA	85	15	0
3.	C85-WMP	85	0	15

Note: *The mix was designed for compressive strength of 25 MPa. In each mix, w/b ratio was kept constant at 0.45 and SP (%) was kept at 1%*

Table 3.1.2: *Mix Design for mortar wythes*

Serial	Formulations	Cement (kg/m3)	SCM (kg/m^3)	Fine Aggregate (kg/m^3)	Water (kg/m^3)	SP (kg/m^3)
1.	C100	546	0	1690	245.7	5.5
2.	C85-FA	464	81.5	1690	245.7	5.5
4.	C85-WMP	464	81.5	1690	245.7	5.5

3.2 Experimental Program for Casting of Panels

A total of 6 specimen were prepared in the experimental program. The samples were scaled down to one-fourth of their original panel size. The dimensions of the panels were 762mm by 305mm and the total thickness of the panels was 180mm.

The total components of a typical specimen are shown in Table 3.2.1**.** Figure 3.1 shows the dimensions and configuration of longitudinal wire-mesh reinforcement in the panel specimen. Figure 3.2.2 shows the detailed cross-section including extended reinforcementdetails of the wall-specimen.

Table 3.2.1*: Panel Sample Components and Dimensions*

Panel Layer	**Type**		**Thickness (mm)**
Mortar Face Wythes	MP-15 Mix Formulation (28 MPa)		50
Insulation Core	15 kg/m3 EPS		80
Panel Reinforcement	**Type**	**Ø Diameter (mm)**	**Spacing (mm)**
Shear Connectors	Steel	3	120
Longitudinal Reinforcement	Steel	2.5	65

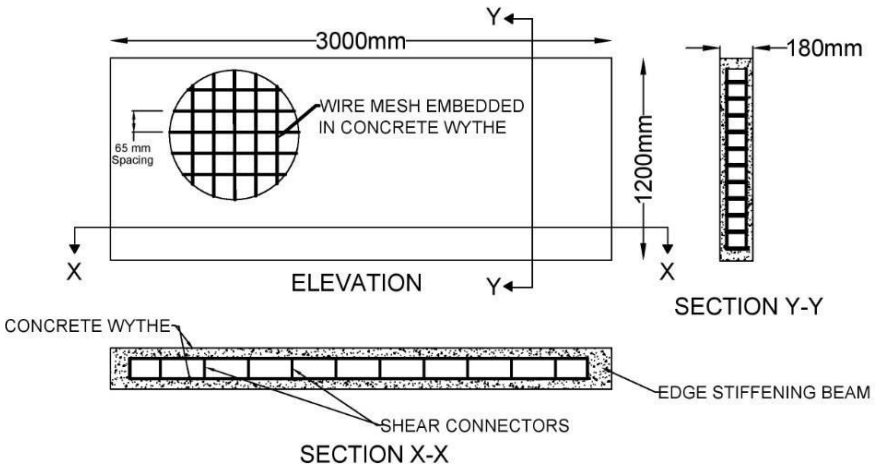

Figure 3.2.1: *Dimensions of Panel and Configuration of Wire-mesh*

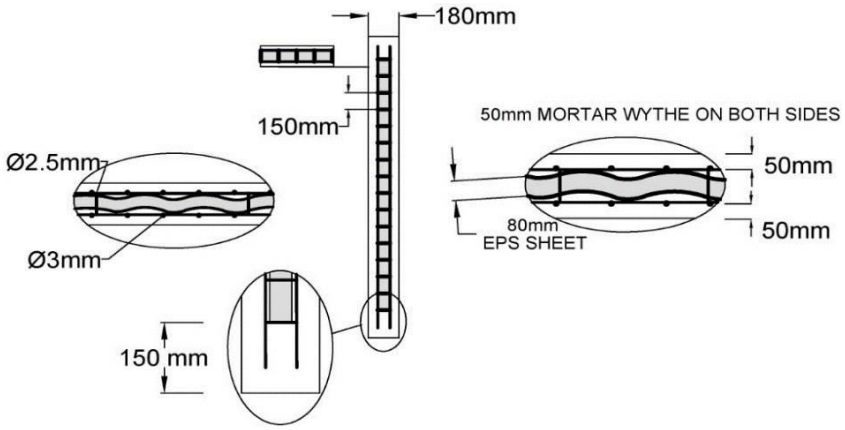

Figure 3.2.2: *Cross-section of panel with extended reinforcement details*

3.3 Materials

3.3.1 Cement

Bestway Cement, which is an Ordinary Portland Cement conforming to ASTM C 150 [28] was used. The chemical composition of the Cement, Fly Ash (FA) and Waste Marble Powder (WMP) are summarized in Table 3.3.1, whereas the physical properties of Cement, FA and WMP are summarized in Table 3.3.2**.** The cement had a specific gravity of around 3.15.

Table 3.3.1: *Chemical composition of Cement, WMP and FA*

Sr. No	Chemical Composition	Cement (% by Weight)	Fly Ash (% by Weight)	Waste Marble Powder (% by Weight)
1.	SiO_2	21	28.03	1.74
2.	Al_2O_3	5.04	14.72	0.71
3.	Fe_2O_3	3.24	7.36	0.31
4.	CaO	61.7	27.19	51.12
5.	MgO	2.56	1.11	2.15
6.	K_2O	0.51	0.45	0.08
7.	Na_2O	0.57	0.06	0.00
8.	SO_3	1.51	2.31	0.02
9.	Cl	0.002	0.007	0.004

***Table 3.3.2**: Physical composition of cement, waste marble powder (WMP), and Fly Ash (FA)*

Sr. No	Physical Property	Cement	Fly Ash	Waste Marble Powder
1.	**Appearance**	Greyish Powder	Black Powder	Off-Whitish Powder
2.	**Specific Gravity**	3.05	3.18	3.12
3.	**Passing Sieve No.**	-	#350	#200
4.	**Blaine Fineness (cm2/gm)**	3650	4400	4050
5.	**Normal Consistency (%)**	27	-	-
6.	**Initial Setting Time (min)**	160	-	-
7.	**Final Setting Time (min)**	210	-	-
8.	**Location**	Bestway Cement	Kohinoor Textile Mills Pvt. Ltd. Islamabad	Commercial Supplier in Sialkot

3.3.2 Fly Ash

The Fly Ash (FA) powder used in the study was obtained from Kohinoor Textile Mills Pvt. Ltd, located in the periphery of National University of Sciences and Technology (NUST) H-12 Campus, Islamabad, Pakistan. The sample obtained was first allowed to dry in sunlight for one day to dry off any surface moisture. After one day of drying, the Fly Ash was passed through a series of sieves and the sample passing through sieve #350 (45 µm) was stored. X-Ray Fluorescence (XRF) spectrometer was used by Bestway Cement Limited to conduct the XRF Analysis of the sample to determine the chemical composition of the samples. The summary of the chemical and physical properties of the Fly Ash sample is shown in Table 3.3.1 and Table 3.3.2. The physical, as well as chemical properties of the Fly Ash sample meet the ASTM C-618-19 requirements of pozzolanic materials [29]. Moreover, the Fly Ash can be classified as a Class C Fly

Ash based on ASTM C-618-19, as the sum of the percentages of Al_2O_3, SiO_3 and Fe_2O_3 is greater than 50% and the percentage of CaO is greater than 20% [29]. The Calcium content of the Fly Ash is said to be the best indicator of how the Fly Ash will behave in concrete (Thomas, 1999). High Calcium fly ashes which Cao > 20% may be produced from lignite or sub-bituminous coals and will react more rapidly than low-calcium fly ashes and renders the fly ash both pozzolanic and hydraulic properties. In addition to providing an indication of the mineralogy and reactivity of the fly ash, the percentage of Cao is also helpful in predicting how effective the fly ash will be in terms of reducing heat of hydration (Thomas, 1995) [30]. Based on the CSA Specific for Fly Ash, the fly ash can befurther categorized as a Type CH fly ash [31]

3.1.1 Waste Marble Powder

The Waste Marble Powder (WMP) used in the study was obtained from a commercial supplier in Sialkot, Pakistan. The sample obtained was allowed to dry in sunlight for one day and then allowed to pass through a series of sieves. The sample pasting through sieve #200 (75 µm) was stored to be used in the mix formulations later. The XRF analysis was used to determine the chemical composition of WMP and based on the requirements of ASTM C-618, WMP is not a natural pozzolan [29]. The percentage of CaO in WMP sample is greater than 50%, which may indicate that it may induce cementitious properties and may be an adequate cement replacement to improve economy, when used in smaller percentages [32]. The chemical and the physical properties of WMP are indicated in Table 3.4 and Table 3.5.

3.1.2 Admixture

MasterGlenium 51, a third-generation superplasticizer which is an aqueous solution of modified poly-carboxylate ether (PCE) polymer, was used in the current study. The sample was in aqueous form and conformed to the ASTM C494-86 standards [34]. The properties of the admixture are present in Table 3.3.3

Table 3.3.3: *Properties of Admixture*

Serial	Parameter	Property
1.	Form	Liquid
2.	Color	Brown Liquid
3.	Specific Gravity	1.10 ± 0.03 g/cm^3
4.	Water Reduction	≥ 112% of Reference mix
5.	Shelf Life	12 months
6.	Max. Dosage (by mass of binder)	0.2-1%

3.1.3 Fine Aggregate

The fine aggregate used for mortar mix recipes was river sand. The sieve analysis of the fine aggregate was performed in accordance with ASTM C 136-04 [36]. The results of the sieve analysis compared with the requirements of ASTM C33-03 [37] and are tabulated in Table 3.3.4. The physical properties of the fine aggregate are summarized in Table 3.3.5.

Table 3.3.4: *Sieve Analysis Results for Fine Aggregate*

ASTM Sieve No	Percentage Retained (%)	Cumulative Percentage Retained (%)	Cumulative Percentage Passing (%)	ASTM Range C-33
#4	3.78	3.78	96.21514	95-100
#8	9.76	13.55	86.45418	80-100
#16	19.92	33.47	66.53386	50-85
#30	39.64	73.11	26.89243	25-60
#50	20.02	93.13	6.87251	10-30
#100	5.38	98.51	1.494024	2-10

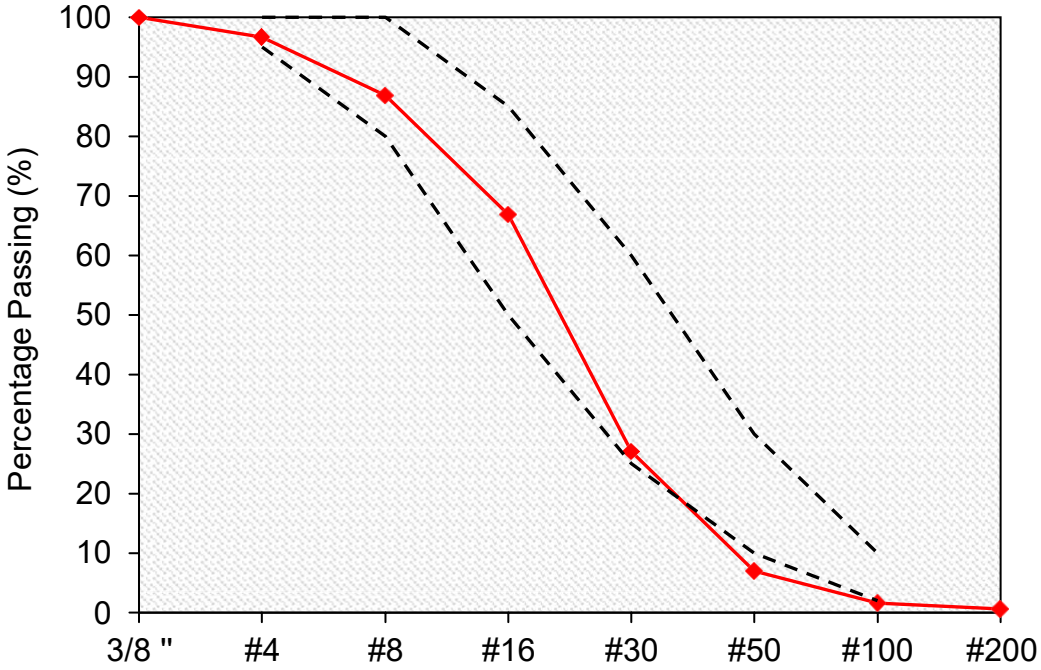

Figure 3.3.1: *Results of Sieve Analysis*

Table 3.3.5: *Physical Properties of Fine Aggregates*

Serial	Parameter	Value
1.	Fineness Modulus	3.16
2.	Bulk Specific Gravity (OD)	2.67
3.	Bulk Specific Gravity (SSD)	2.70
4.	D50 (mm)	0.9
5.	Absorption (%)	1.21%
6.	Quarry	River Sand

3.1.4 Expanded Polystyrene

The insulation used for the panels was a low-density Expanded Polystyrene (EPS) insulation and was provided by Sustainable Housing Solutions (SHS). The density of the EPS core 15 ± 3 kg/m^3 and the thermal conductivity of the EPS as specified by the manufacturer is 0.039 W/m.K. The material properties of the EPS core are detailed in Table 3.3.6.

Table 3.3.6: *Material Properties of EPS*

Serial	Parameter	Value
1.	Nominal Density	15 ± 3 kg/m^3
2.	Thermal Conductivity	0.039 W/m.K
3.	Fire Rating (UNE-EN 13163:2013) [35]	E
4.	Dimensional Stability	± 5%
5.	Flexural Strength	≥ 112 kPa

3.1.5 Steel Wire

Galvanized Smooth Steel Wire was used for longitudinal reinforcement and shear connectors in the panels. The nominal diameter of the wire was 3mm and the ultimate tensile strength was 700 MPa as specified by the manufacturer. The detailed specifications of the steel wire are tabulated in Table 3.3.7.

Table 3.3.7: *Specifications of Steel Wire*

Serial	Parameter	Value
1.	Nominal Diameter	Ø 2.5 and Ø 3 mm
2.	Yield Strength	650 MPa
3.	Tensile Strength	700 MPa
4.	Elongation at Maximum Load	2.5%
5.	Mass of Welded Fabric	Ø2.5 mm: 0.0358 ± 6% kg/m Ø3.0 mm: 0.0555 ± 6% kg/m
6.	Resistance to Corrosion	Zinc Coating Class D

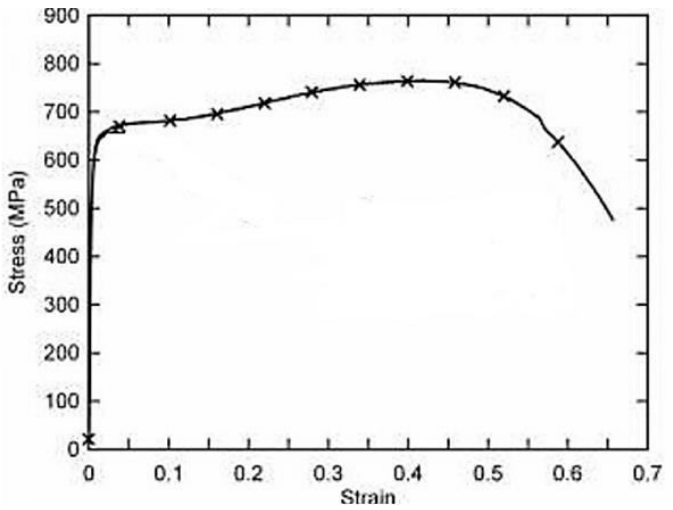

3.2 Mixing Regime, Casting and Curing

3.2.1 Mortar Samples

ASTM C 305-14 [38] standard was adopted for the mixing regime to ensure that all samples were prepared with the same uniformity in a 5 L capacity Hobart Mixer. At first, all the dry ingredients of the paste, namely cement and SCM, were manually mixed in a small container. The dry mix powder was then fed into the container of the Hobart mixer, followed by the required amount of water mixed with superplasticizer (SP). The dry mix was allowed to be absorbed in the water-superplasticizer mix for 30 s. At first, the batch was allowed to mix for 30 s at (140 ± 5 rev/min) and then the mixer was stopped for 15 s to scrape off any excess paste material that adhered to the sides of the container. Thereafter, fast mixing (285 ± 10 rev/min) was conducted for 60 s before the mix was finally really to be poured in molds. The fresh mix was immediately poured into molds of various size and shapes required for the different tests: 50 mm cubes, 40 mm x 40 mm x 160 mm prisms, 25 mm x 25 mm x 285 mm prisms, 100 mm x 200 mm cylinders. The samples were left to harden for 24 h in the casting room at room temperature. The following day, the samples were de-molded and immersed in a 1000 L curing tank at a temperature of 24 ± 2 ◦C. The curing facilities used meets the requirements of ASTM C-511 [39] and samples were cured as per requirements of ASTM C-192 [40] before they were taken out for required testing. The water for curing of shrinkage samples was lime-saturated water to avoid leaching out of Calcium hydroxide from the samples. The sample were taken out of the curing tank and allowed to air-dry for one hour prior to their testing. A total of 36 cubes, 36 flexure test prisms, 9 drying shrinkage prisms and 12 cylinders were casted for different tests.

3.2.2 Casting and Curing of Panels

A total of 6 specimen were prepared in the experimental program. The samples were scaled down to one-fourth of the original panel size for testing in compression and shear. The small-scale panels were tested to determine the local compressive strength of the panels. The height of the specimens was 762mm and their corresponding length was set at 305mm. Essentially, the aspect ratio of the panels is kept as 2.5, the same as full-scaled panels. The total thickness of the panels was 180mm. 50mm mortar wythes made of normal strength mortar with 28MPa compressive strength were used for both

mortar wythes. In addition, an 80mm low-density Expanded Polystyrene (EPS) insulation layer was used as the core layer in the panels.

A 65mm square reinforcing mesh composed of smooth galvanized steel bars with 3mm diameter was placed with a cover of 15mm from the exterior sides of the mortar wythes. Shear connectors made from the same material and 2.5mm in diameter were placed and welded to the longitudinal reinforcing meshes at 90°, and at every 225mm on the width and at every 75mm on the length of the panels.

The specimens were prepared casting using the following methodology: System of steel wire-mesh reinforcement was placed on both sides of the EPS core insulation. Shear connectors were inserted into the EPS core and allowed to penetrate to the other side of the core. Electric welding was utilized to weld the steel shear connectors to the steel wire-mesh longitudinal reinforcement to create an effective system for transfer of shear between the mortar wythes.

The panels were cast in mold made from wooden cardboard as shown in the Figure 3.4.1 (a) and (b). The mixing of the mortar was done in a 108 L Pan mixer and mixing was done conforming to requirements of ASTM C 305-14 [38] standard. The casting of the panels was done by placing a single layer of mortar on the EPS core and allowing it to set for one-day and then flipping the side of the panel and placing the other mortar layer on top of the EPS core. Figure 3.4.2 (a), (b) and (c) show casting and curing of scaled wallpanels

(a)

(b)

Figure 3.2.1: (a) and (b): *Wooden cardboard used as molds for casting of panels*

(a) (b) (c)

Figure 3.2.2: *(a) Casting of layer of mortar wythe (b) Mortar Wythe after setting for one day (c) Curing of scaled wall panels*

In addition to samples for compression, one sample with dimensions 1500 mm by 1200 mm was casted utilizing similar reinforcement as that of compression sample, to be tested in flexure. The layer thicknesses and mix recipe used was like samples used for compression. The slab panel was casted in a similar fashion to scaled wall samples, with one side of the slab panel concreted first and other side of the slab panel concreted the following day. The sample was allowed to cure in air for 28-days before it was tested in flexure. Figure 3.4.3 (a) and (b) shows casting of slabs panels.

(a) (b)

Figure 3.2.3: *(a) and (b): Casting of 5' x 4' Slab Panel*

3.3 Ecotect Thermal Comfort Analysis for Cooling Loads

The aim of this analysis was to investigate and compare the potential reduction in electricity usage by utilizing concrete sandwich panels in residential buildings compared to traditional R.C.C and brick masonry residential construction. Hence, a 740 ft² single-story residential house was selected for performing the thermal comfort analysis. The architectural layout of the house used to perform thermal comfort analysis was extracted from the Naya Pakistan Housing and Development Authority's (NAPHDA) website, where they have provided architecture layouts of various homes of different sizes and shapes, which are to be constructed in the upcoming Naya Pakistan Housing scheme. The 740 ft² house contains two bedrooms, a large living room, a kitchen, and a small room for storage. The plan view of the house is shown in Figure 3.5.1.

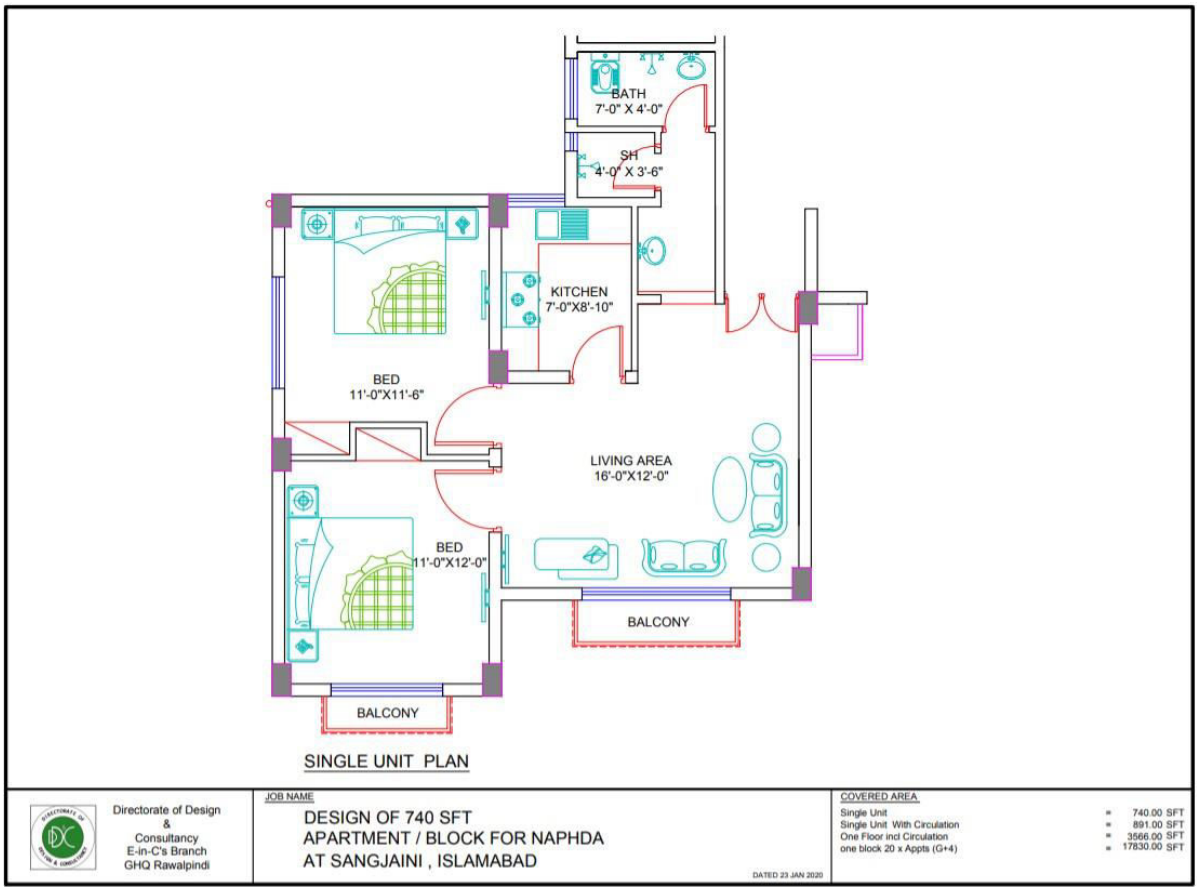

Figure 3.3.1: *Plan View of 740 ft² single-story house (Source: Naya Pakistan Housingand Development Authority Website)*

3.3.1 Building Envelope

Before modelling a house and performing thermal analysis on it, it is important to define the main building elements/components of the home. This is known as the building envelope of the building. The main components of the building envelop are the roofs, floors, walls, windows and doors used in the building. Forming a building envelop is important because it is the key component which forms the barrier between the external environmental conditions and the internals ones. Without a building envelope, the internal and the external temperatures would be no different.

After defining the building envelope, a 3D model of the single-story residential building was made in Autodesk REVIT using the main components of the building envelope. In this phase, it is important to define parameters such as building materials, their U-values which can be extracted from thermal conductivity tests and the size, dimensions and architectural placement of rooms and orientation of the house to be constructed. To import a file from Autodesk REVIT, the only primary way of getting the geometry from it is a gbXML. file format. Green building (gb.) extensible markup language (XML) file format helps in converting the rooms, spaces and zones from the Autodesk REVIT software which allows the analysis for different performances such as thermal, acoustic, energy demands and sustainable indexing. The 3D model of the building constructed in REVIT is shown in the Figure 3.5.2**.**

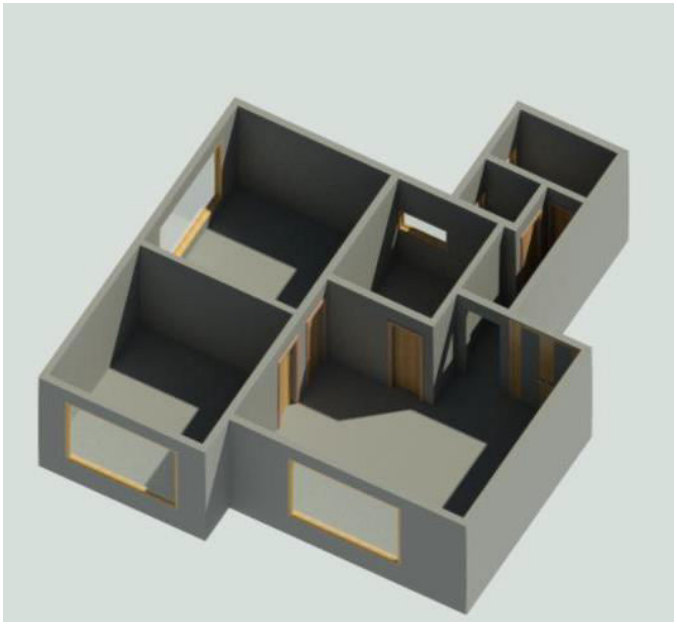

Figure 3.3.2: *3D model of the building constructed in REVIT*

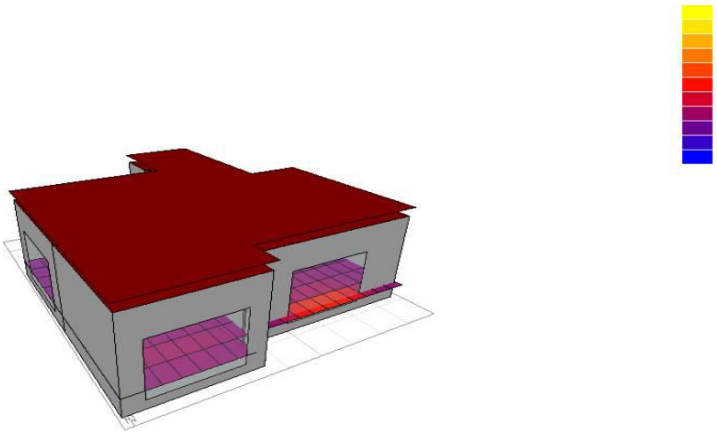

Figure 3.3.3: *Building Model imported from REVIT into ECOTECT software*

To carry out the thermal comfort analysis, the software requires us to set internal parameters and external parameters. The internal parameters include type of HVAC system, number of residents etc. and the information regarding the room dimensions, transmittance values of materials used and room placement is taken from the BIM model constructed beforehand. Moreover, the software also requires us to input external data which mainly includes environmental factors such as:

- Daily/Monthly/Annual Temperatures
- Daily/Monthly/Annual Humidity
- Daily/Monthly/Annual Solar Tracking
- Daily/Monthly/Annual Winds
- Daily/Monthly/Annual Overshadowing
- Daily/Monthly/Annual Daylight

As an alternative to defining the external parameters manually, a weather data file using the gbXML file format, can be extracted from online sources and can be integrated with ECOTECT software. The software uses the weather data file and analyses all the parameters such as temperatures, solar radiations, humidity etc. It converts the data into an energy model. Hence, a weather data file for Karachi at latitude 24°48'N and longitude 66°59'E, 4 m (13 ft) above the sea level, on coast was extracted from climatemps.com [99] and used for the purpose of this study. It is easy to see the potential overheating due to the sun and daylight once we have selected a local data file. The software helps in investigating trends such as wind speeds, cloud covers, temperatures and solar radiations and makes a correlation between these data which helps in analysis.

Table 3.5.1 and Figure 3.5.4 display the summary for the internal parameters of the buildingand external parameters of Karachi used for performing the thermal comfort analysis. Table 3.5.2 displays the summary for the transmittance values of the components of building envelope.

Table 3.3.1: *Indoor Design Conditions as per Weather File of Karachi, Autodesk ECOTECT, 2011*

Parameter	Value
Relative Humidity	60%
Wind Speed	3m/s
Thermostat Range	24°C
HVAC System	Full Air-Conditioning
Air Change Rate	0.50/hr.
Wind Sensitivity	0.25/hr.
Number of persons	4

Table 3.3.2*: Transmittance Values for Building Envelope Components*

No.	Building Components	Conventional U Value (W/m^2K)	Masonry Wall U Value (W/m^2K)
1.	Roof	1.020	1.020
2.	Walls	1.800	2.00
3.	Doors	2.980	2.980
4.	Windows	5.430	5.430
5.	Floor	1.330	1.330

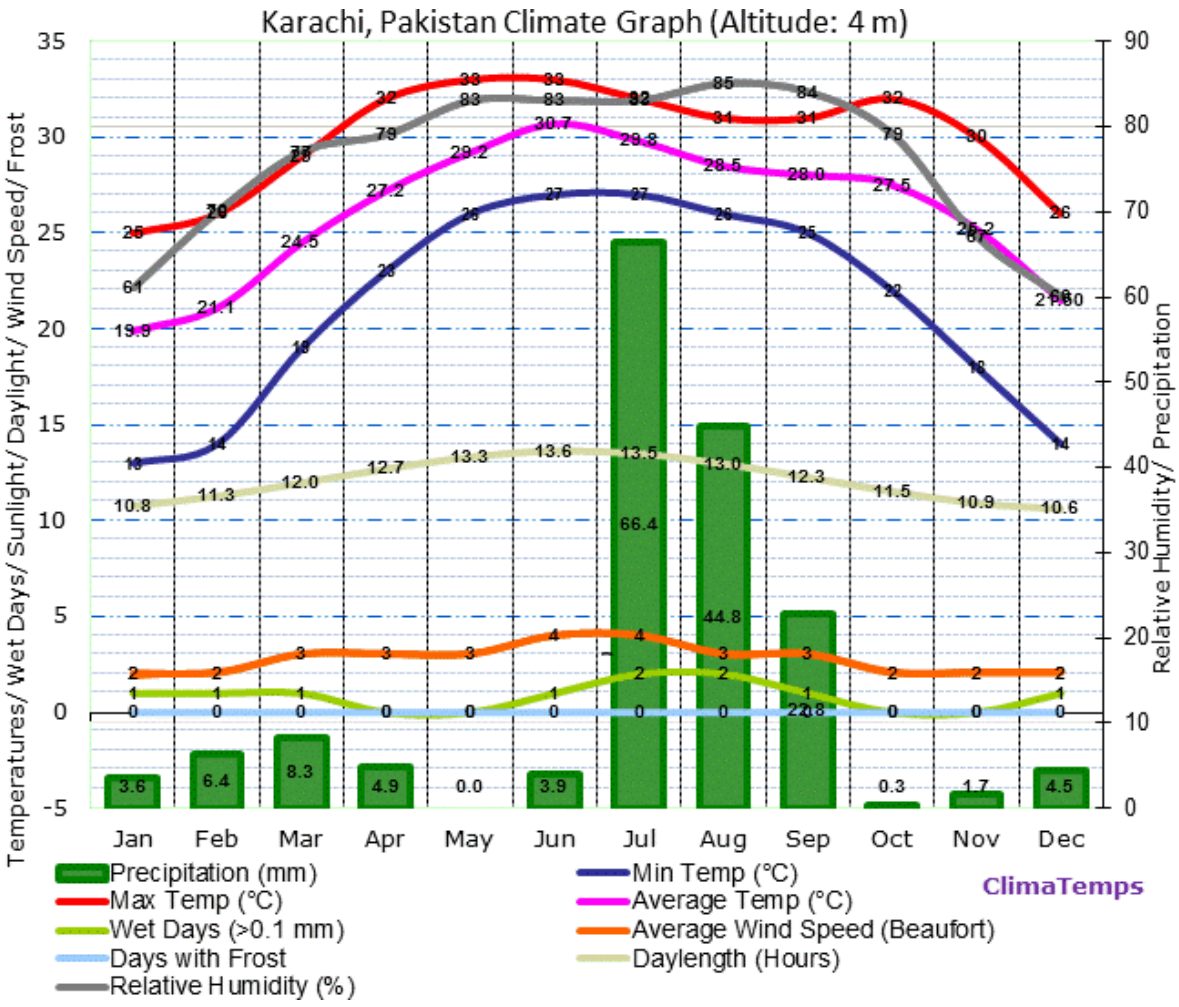

Figure 3.3.4: *Karachi, Pakistan Climate Graph (Altitude 4m). (Source: http://www.karachi.climatemps.com)*

The walls in a typical residential structure can be constructed using brick masonry or concrete blocks. Hence, for the purpose of comparison, walls made of either 9" thick brick masonry with transmittance value of 2.00 W/m²K or 8" thick concrete blocks with transmittance value of 1.80 W/m²K are used for the purpose of comparison with lightweight panels. The transmittance values for rest of the building envelope components are extracted from [71] and extended details for the roofing & flooring materials, windows and doors are given in Table 3.5.3

***Table 3.3.3**: Extended Details for the roofing materials, floor materials, windows and doors*

No.	Building Components and Specifications		Thickness (inches)	Density (kg/m^3)	Conductance (W/mK)
1.	**Roof U Value 1.020 (W/m2K)**	Roof Tiles	1 1/2“	1900	0.840
		P.C.C	2”	950	0.209
		Mud Phuska	3”	1620	0.520
		Bitumen	3/8”	1700	0.500
		Concrete	6”	2300	1.046
		Air Gap	6”	1.3	5.560
		Plaster Ceiling Tiles	3/8”	1120	0.380
2.	**Ground Floor U Value 1.330**	Ceramic Tiles	3/8”	656	0.309
		P.C.C	2”	950	0.755
		Brick Masonry	4”	836	0.711
		Sand	4”	840	1.711
		Soil	9”	1046	0.837
3.	**Concrete Block Wall U Value 1.800**	Plaster	3/8”	1250	0.431
		Concrete Block	8”	1800	1.3
		Plaster	3/8”	1250	0.431

After all the parameters are defined, a thermal comfort analysis is run on the building model and the software then provides us with the comprehensive results of the rating system. It runs calculations based on the criteria and standards provided by the BCAs Energy codes, ASHRAE 90.1, LEED and others similar LCA rating systems.

3.3.2 Embodied Energy

As dictated by literature, around 99% of the embodied energy is consumed during the manufacturing and the operational stage [80]; hence, the scope of this study is limited to finding the embodied energy due to carbon emissions during the manufacturing stage and the operational stage only. The energy consumed during the transportation, construction and demolition is outside the scope of this study. Moreover, the target of this study is to carry out an approximate estimate for the embodied energy rather than an accurate one considering even the most minute of factors:

3.5.3.1 Manufacturing Stage

For the determination of embodied energy, it is possible to use process analysis, input-output analysis, or hybrid analysis. One of the main requirements of the input-output method is the energy used at country level in different sectors of the economy. Such data is not available in Pakistan. Also, this method is not suitable for estimating the energy of individual products. Hence the use of input-output method is not possible. On the other hand, Hybrid method is a combination of process method and input-output method. Hence, hybrid method also cannot be used due to lack of data since it is a combination of input-output method and the process analysis method.

Therefore, process analysis method was used. In this method, the embodied energy of each stage of manufacturing for each ingredient is assessed along with any other energy needed for the production. The embodied energy of individual materials has been obtained from various sources. For example, embodied energy of cement is taken as 0.912 kg CO_2/kg given in ICE (Inventory of carbon and energy) database. The sand used is mined from about 100 km away. A typical embodied energy co-efficient mentioned in ICE database has been used 0.006 kg CO_2/kg for sand. Since it is a very low value, its accuracy will not have much effect on total embodied energy. The embodied energy for admixture is 1.88 kg CO_2/kg. Embodied energy of foam core is high. According to ICE database embodied energy value of EPS core foam is 2.5 kg CO_2/kg, and it was selected for this report, while that of steel wire mesh is 0.269 kg CO_2/kg. The embodied energy for various materials during manufacturing phase is shown in Table 3.5.4.

3.5.3.2 Operational Stage

During the operational stage, there are about five to six factors which contribute to the embodied energy. These factors are illustrated in the Figure 3.5.5, presented by Peng, 2016; Yang et al., 2018 [101, 102]. Since the scope of this study is to illustrate the reduction in CO_2 emissions brought about by use of sandwich panels, the only apparent reduction in CO_2 equivalent will be because of reduced electricity usage due to cooling loads; hence, only HVAC will be considered as the basis for comparison in the operational stage.

***Table 3.3.4*:** *Embodied Energy for various materials during their manufacturing as mentioned in ICE database.*

Sr No.	Material	Energy Intensity
		Kg-CO_2/kg
1.	Cement	0.912
2.	Fly Ash	0.004
3.	Sand	0.006
4.	Aggregate	0.00747
4.	Plasticizers	1.88
5.	Burnt Clay Brick	5.502
6.	Lime Mortar	0.891
7.	EPS Foam	2.5
8.	Steel Wire Mesh	0.269

The methodology employed to calculate the embodied energy because of cooling load will simply consist of determining the carbon emissions from power sector in units of CO_2/MWh and multiplying this value by the cooling load determined from the thermal comfort analysis of the building using ECOTECT software.

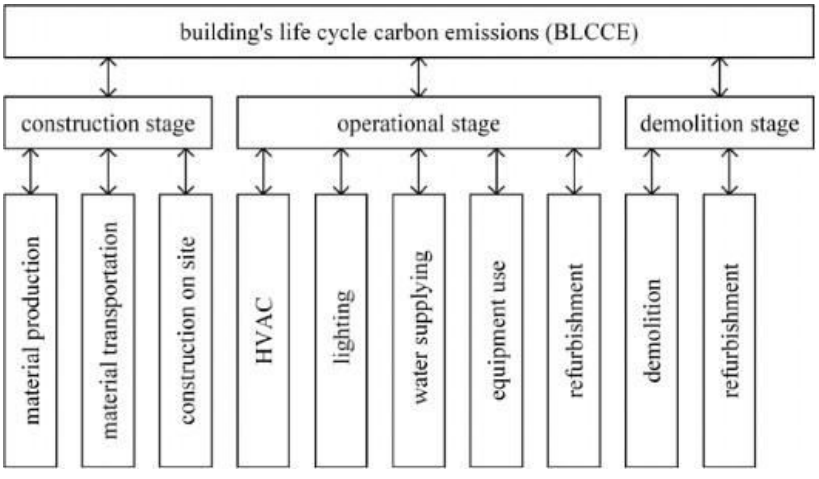

Figure 3.3.5: *Composition of a building's life cycle Carbonemissions*

CHAPTER 4: EXPERIMENTATION

4.1 Mortar Tests

4.1.1 Flowability

Flowability is an important parameter that provides a general idea about the characteristics of fresh mortar paste. The purpose of finding flowability is to determine and optimize the water to binder ratio (w/b) and percentage of superplasticizer in the mortar paste based on a specific flow level. Flow Table Test was used to determine the flowability of the sample and the test was performed as specified by ASTM C-1437 [42]. Flow Mold with 100 mm base diameter and flow table apparatus was setup as specified in ASTM C 230 [41]. The fresh mortar mix was poured into the flow mold at room temperature in 25 mm layers and tamped 20 times with tamper. The table was allowed to drop 25 times in 15 s and the average diameter of the resulting flow was measured using a ruler. The flow test was repeated three time for each mix formulation and determined using the following formula:

$$E\% = 100\frac{D_f - D_i}{D_i} \quad (1)$$

where:

E: Flow expressed as a percentage (%),
D_f: Final diameter (cm),
D_i: Initial diameter (cm).

4.1.2 Mechanical Strength

The compressive and flexural strengths of the mortar formulations were determined by procedure described in ASTM C-348 [43] and ASTM C-349 [44]. Compressive strength at any age is the average of three 50 mm cube samples, whereas the flexural strength at any age is the average of three 40 mm x 40 mm x 160 mm prism samples. The samples were tested for their mechanical strength at age 7, 14 and 28 days.

4.1.3 Drying Shrinkage

Drying shrinkage determines the change in length of the mortar test specimen as it ages, where by length change me be induced by externally applied forces due to changing temperatures, relative humidity and evaporation of water from the capillary pores of

specimen or due to heat of hydration as mortar ages; drying shrinkage is the net effect of length changes due to all external forces and internal forces [45]. Drying shrinkage is an important parameter to determine because loss of capillary water results in cracking, which brings significant reduction in durability and mechanical strength of the specimen. For mortar specimens, drying shrinkage is more pronounced when compared to concrete, due to the larger quantity of cement used per unit volume; cement being the heat releasing agent in concrete.

The test was performed at 24 ± 2 ◦C room temperature and 100% humidity, using a 25 mm x 25 mm x 285 mm prisms specimens and procedure followed for testing was as specified in ASTM C 596-01 [46]. The test specimen was cured in moist conditions along with the mold for 24 h, after which it was demolded and cured in lime-saturated water for 48 h. After immersing the sample for 48 h in lime-saturated water, the specimen was air-cured for remaining age and length comparator readings were obtained after 4, 11, 18 and 25 days of air storage.

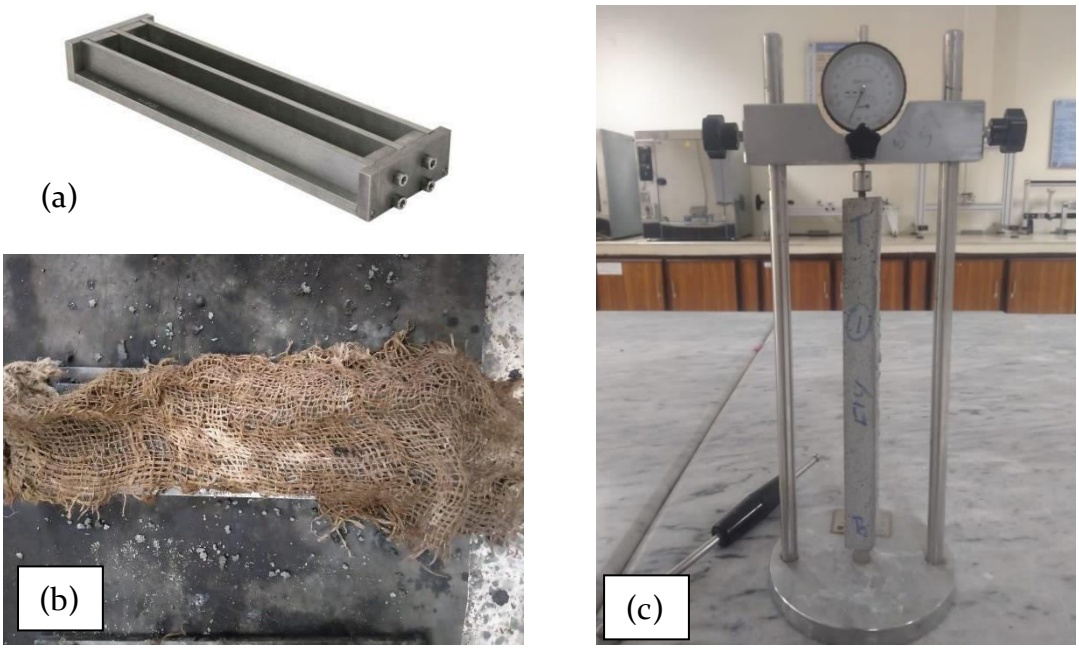

Figure 4.1.1: *(a) Mold for Shrinkage Test (b) Curing of shrinkage test molds (c) Shrinkage mold setup in shrinkage apparatus*

4.1.4 Electrical Resistivity of Mortar

Electrical resistivity test of concrete is also known as Rapid Chloride Penetrability (RCP) test for concrete and is used to assess the durability of concrete [49]. It is an important

test which gives an indication of the chloride Ion penetrability potential of concrete. The test method measures the total electrical charge passing through the cylindrical specimen of concrete or mortar, subjected to a standard voltage. RCP provides an insight to the potential of a mortar specimen to resist penetration of chloride ions but it is not capable of direct measurement of chloride penetrability [49]. The test method is standardized as ASTM C1202 [48] and AASHTO T-227 [50]

Chloride Ion penetration is an important parameter to determine as chloride ions can lead to corrosion of steel in R.C.C structures and hence, affect the durability of the overall structure [47]. Since the cover provided for galvanized steel wire-mesh in the casted sandwich panel is 15 mm, it is important to assess whether the mortar is durable enough to resist the penetration of chloride ions. The electrical resistivity or RCP test works on the principle that durability of concrete depends on porosity and microstructure of the specimen. A finer pore network, with less interconnectivity results in a low permeability concrete and vice-versa. Hence, electrical resistivity of concrete can be defined as the ability of concrete to withstand transfer of ions when subjected to an electrical field [48].

For this research, the two-point uniaxial test method was chosen to measure the electrical resistivity of the mortar sample, which involved placing a mortar or concrete cylinder between two electrodes (which are usually parallel metal plates) with moist sponge contacts at the interfaces to ensure a proper electrical connection. CMT Digital Resistivity Array Meter was used to measure the resistivity of the mortar specimen. The test set-up for uniaxial electrical resistivity test is shown in Figure 4.1.2 (a) and (b)

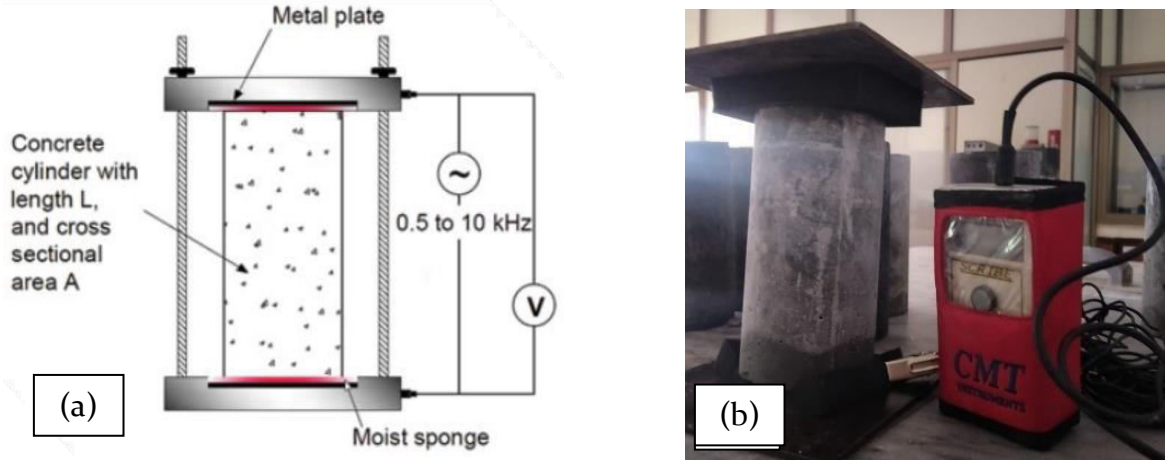

Figure 4.1.2 (a) and (b): *Test set-up for Uniaxial Electrical Resistivity Test*

4.1.5 Carbonation

Carbonation is another important perimeter to determine the durability of test specimen. Concrete carbonation is a serious menace for the durability of concrete structures as carbonation can bring about reduction in pH of concrete, de-passivation of deactivated film of reinforcing bar, cracking of concrete cover [52] and decomposition of hydration products to form by-products such as Calcite and water from carbonation of Calcium Hydroxide (CH), Calcite, Silica Gel and water from Calcium Silicate Hydrate (CSH) and Calcite, Alumina Gel and water from Calcium Aluminate Hydrate (CAH) [51].

Petrographic examination at ages one, two and three months was performed after 28-day aging of mortar. The 100mm x 200mm mortar cylinder specimen was cut down to form three equal cylindrical specimen with diameter of 100 mm and depth of 66.67 mm and the exposed surface, that is, the circular cross-section of the test specimen was sprayed with phenolphthalein alcoholic solution. The solution remains clear on the carbonated portion of the concrete but turns pink where the exposed surface remains uncarbonated. This test method works on the principle of measuring the pH of concrete surfaces, as carbonations tends to reduce the pH of the exposed mortar surface [51]. The sprayed samples were viewed under a microscope having a least count of 0.01 mm, to detect signs of carbonations on the exposed surface of the samples.

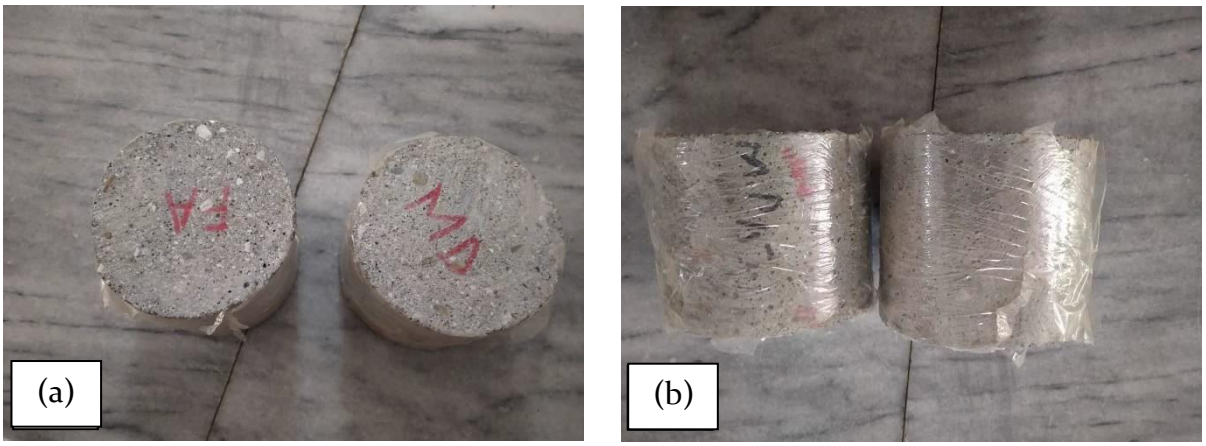

Figure 4.1.3: *(a) 100mm diameter by 66.67mm height sample after being sawed down (b) Curved Surface area of the sample wrapped in plastic sheet to prevent carbonation through surface area*

4.2 Sandwich Panel Tests

4.2.1 Thermal Transmittance (U-Value)

Thermal Transmittance is defined as the rate of transfer of heat through a matter. U-Value or thermal transmittance is used to determine the thermal efficiency of a specimen. For the determination of thermal resistance of a wall panel specimen, Heat Flow Apparatus was used and test procedure conforming to ASTM C518-15 [53] and ASTM E 1530-99 [54] was followed. The test and analysis of test results were conducted in U.S-Pakistan Center for Advanced Studies in Energy (USPCAS-E), NUST and the results of thermal transmittance was reported.

The test setup involves the specimen being placed between a hotplate and a cold plate and heat flux transducers. The temperature range for testing was 0◦C to 50◦C, which is a representation of the maximum and minimum temperatures in Islamabad, Pakistan. The testing assembly is shown in Figure 4.2.1 [53].

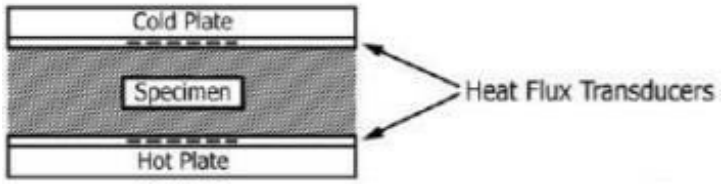

Figure 4.2.1: *Test Assembly for Thermal Conductivity Test*

4.2.2 Compression Strength

The casted specimens were allowed to cure for 28-days, before they were tested for their compressive strength in the compression testing machine at NICE Structure Laboratory, National University of Sciences and Technology (NUST). To assume a uniform load distribution, steel caps/plates were placed at the upper cross-section of the panel, which was in contact with the hydraulic press of the compression testing machine. The test assembly is shown in the Figure 4.2.2 (a) and (b).

While testing, a jack in the compression testing machine applied compressive load at a rate of 0.25 MPa/second to a 3cm thick steel plate which was in contact with top and bottom surface in the orientation the compressive loads was applied in and strain gauge dial was used to manually determine the length changes at various time intervals

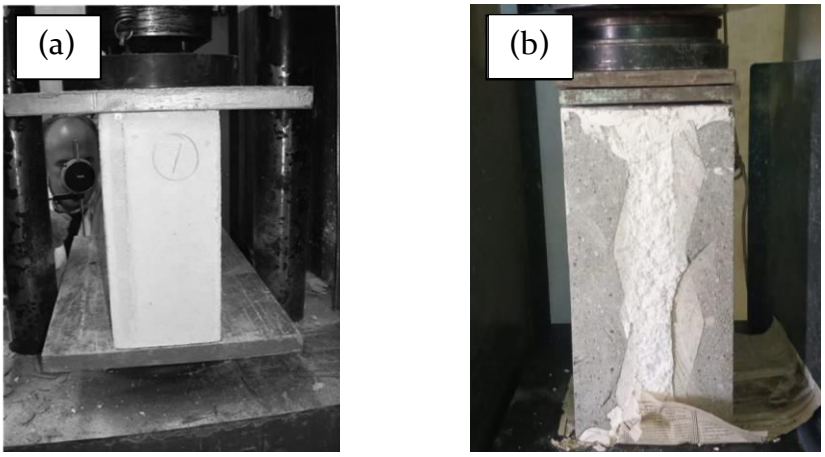

Figure 4.2.1: *Test Assembly for compression testing of scaled wall panels*

4.2.3 Flexural Strength

The dimensions of the specimen casted for flexure strength test was 1500 mm by 1200 mm and the specimen was 186 mm in thickness. The slab panel was allowed to cure for 28-days by water curing by splashing a thin film of water on the surface of slab panel and then rotating the panel daily by 180 degrees to cure the other side of the panel. The slab panel specimen was tested in three-point bending in reaction chamber at for determining the flexural strength of the slab panel. The test setup for three-point bending is shown in Figure 4.2.3. A hydraulic press was used to apply pressure at a rate of 0.25 MPa/sec on a beam which was resting on top of the slab panel to apply a uniform line load across the centerline of the slab panel. The slab panel was simply supported by resting it on top of two roller supports. The slab panel was loaded until first crack developed at the bottom layer of the sandwich panel configuration.

Figure 4.2.3: *Test Setup for three-point bending test of slab panel*

CHAPTER 5: RESULTS AND DISCUSSION

5.1 Flowability

The results of flowability for all four mix formulations are tabulated in Table 5.1. The percentage of superplasticizer was adjusted until a constant flow of 210±10 mm or 110±10% was achieved at water/binder ratio of 0.45 by the control mix (C100) so that it conforms to ASTM C270 [33] standards. With the addition of 15% Fly Ash (FA) by weight of cement, it is observed that the flow percentage decreases by 9% and a further 10% replacement of cement by Fly Ash results in an additional 5% reduction in flow. Fly Ash particles have a greater surface area than cement particles as determined by Blaine Fineness Test results (Table 3.3.2); and hence, because the fly ash particle is finer than cement, the water demand of the resulting mixture increases as the percentage of Fly Ash (FA) in the mix is increases [56]. The WMP mix displays a similar trend with the flow percentage decreasing with the addition of WMP in the sample. At 15% weight replacement, WMP mixture has 3% greater flowability value when compared to FA mix, due to the lower Blaine Fineness of the WMP sample [56].

According to [62], using WMP with a higher Blaine Fineness in the manufacturing of concrete causes in a decrease of the workability and an increase in the friction.

***Table 5.1.1**: Results of Flow Test*

Serial	Formulation	Average Flow Diameter (mm)			Average Flow (mm)	Flow Percentage (%)
1.	C100	209	212	210	210.33	110%
2.	C85-FA	201	202	202	201.33	101%
3.	C75-FA	195	195	199	196.33	96.33%
4.	C85-WMP	207	204	201	200	104%

5.2 Mechanical Strength

The compressive and flexural strengths at ages 7, 14 and 28 days are shown in figures 5.2.1 and 5.2.2. The results indicate that Fly Ash (FA) mix recipe has almost 13-15% lesser strength when compared to control mix at all ages. This decrease in compressive strength may be attributed to the following reasons: the effective water to cement ratio

increased with an increase in fly ash replacement level and the pozzolanic reaction is also a slow reaction. It requires more time for complete reaction to take place to attain a higher strength than controlled specimen; hence, adding fly ash brings a change in strength by two principles: the dilution effect and the chemical effect on cement hydration. The dilution effect is a consequence of the replacement of cement by fly ash, which equates to an increase in water/cement ratio [57, 58]. Whereas the chemical effects represent the strength increase as a result of the reaction between mineral admixture and calcium hydroxide which produces fibrous CSH. At 15% replacement of cement by Fly Ash, the dilution effect dominates the chemical effect; and thus, a decrease in compressive strength up-to 28-day age is observed. The pozzolanic reaction between mineral admixture and Calcium Hydroxide (CH) takes places after 28-day age, which is not studied in the scope of this research [58]

The utilization of WMD at 15% replacement led to a decrease of 8% in the 28-day age compressive strength, whereas the 7- and 14-day age compressive strength results were much comparable. The similarity in the compressive strength at early age is because cement and WMP have compare CaO; a compound which helps speed up the hydration process. But as the concrete ages, it requires Silica to continue hydration such as in

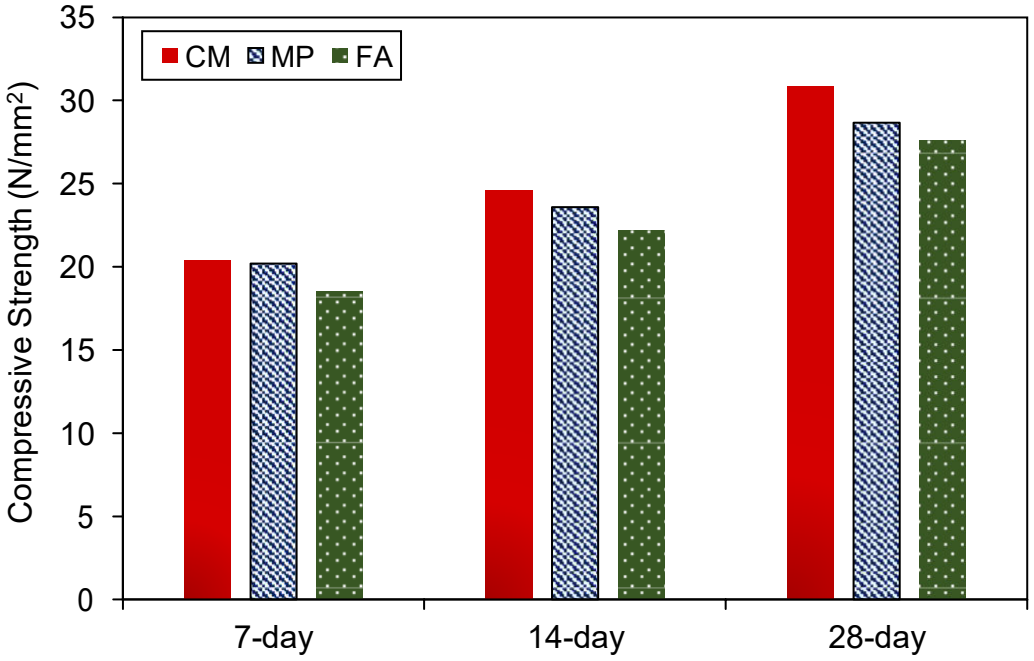

Figure 5.2.1: *Compressive Strength Test Results for Control Mix (CM), Marble Powder Mix (MP) and Fly Ash Mix (FA)*

pozzolans. The decrease in compressive strength proves that WMP does not possess pozzolanic properties and thus, reduces the effectiveness of the hydration process [59, 60, 61].

The results of the flexure strength test indicate that WMP mortar mix has the least flexural strength out of the three mixes, whereas the results of control mix and FA mix are much more comparable. According to [58], when analyzed under a Scanning Electron Microscope (SEM), the microstructure of the WMP shows a higher content of unreacted calcium hydroxide (CH) and analyzing the images of hydration products at various ages, it is revealed that the percentage of calcium hydroxide (CH) in the pore structure increases with the addition of WMP by percentage of cement. [58] emphasizes that this can be explained by water accumulating around WMP particles, which result in a reduction in the water requirement and therefore, results in increased porosity of the microstructure. In addition, the Calcite provided by WMP reacts with tricalcium aluminate of cement to form calcium carbo-aluminates [63, 64]; but the lack of silicates and aluminates in the WMP results in lesser CSH as hydration products [58].

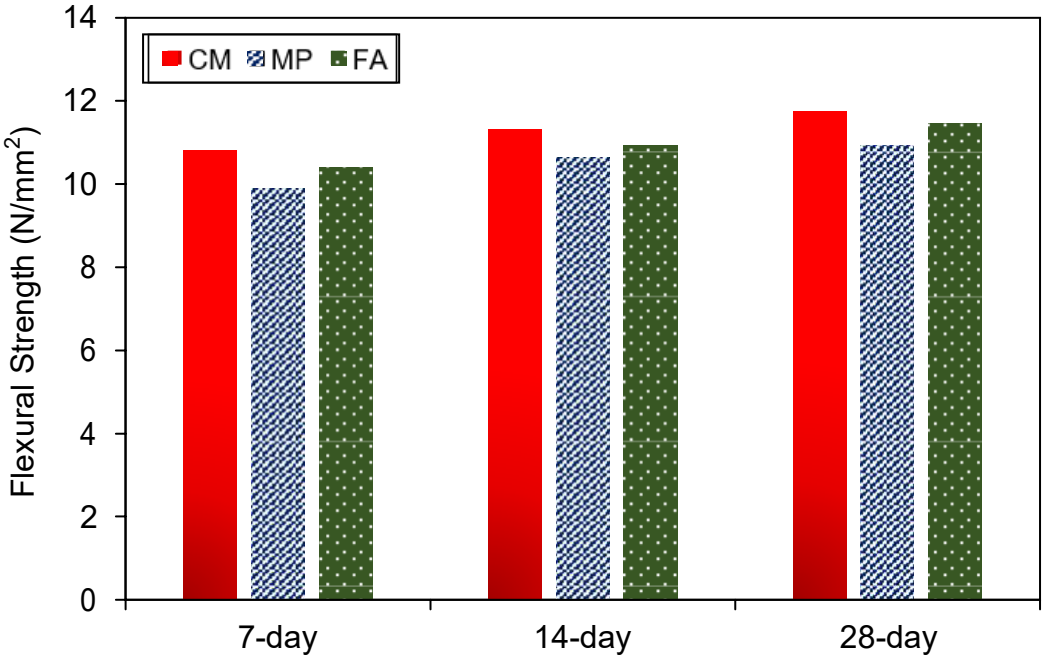

Figure 5.2.2: *Flexure Strength Test Results for Control Mix (CM), Marble Powder Mix (MP) and Fly Ash Mix (FA)*

5.3 Shrinkage

The drying shrinkage test was performed according to ASTM C 596-01 [46] and the readings were noted for 4, 11, 18 and 25 days. The results of the shrinkage test reveal that the drying shrinkage for the three specimen is below 250 micrometers, which is well below the limit of 600 micrometers specified by ASTM C 157 [65] and AS 3972-2010 [66]. Moreover, the test results also highlight the control mix having the greatest length change due to drying shrinkage, followed by WMP mix and lastly FA mix. These test results can be explained by the heat of hydration emitted during the hydration process of each formulation.

The reason for the low heat of hydration is a result of the dilution effect because of mineral admixtures replacing cement in the paste. At early ages, silicates, and aluminates in the mix need tricalcium silicate to react with, but at 15% replacements, C_3S is not adequate to completely react with all the hydration reactants in the FA mix [67]. As for later stages of hydration, the percentage of calcite decreases in the mix paste, which reduces or effects the performance of hydration and production of calcium hydroxide (CH). Hence, the drying shrinkage of Fly Ash mix is the lowest among the mix formulations, followed by WMP mix.

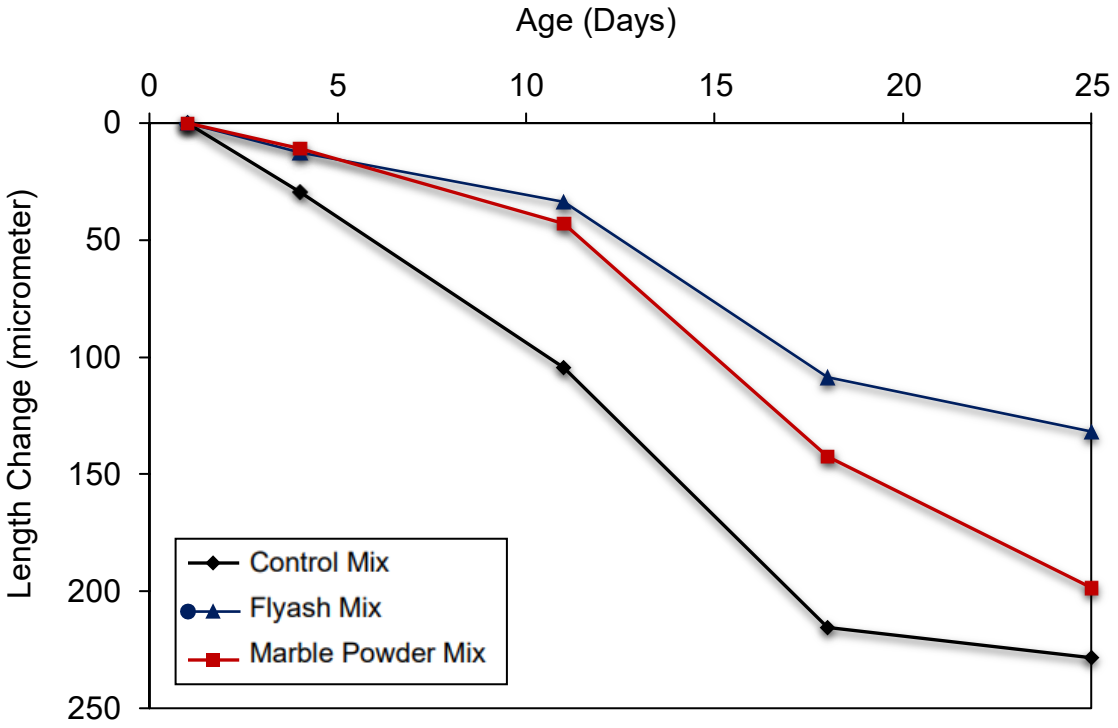

Figure 5.3.1: *Shrinkage Test Results*

5.4 Electrical Resistivity

The electrical resistivity test was performed using the Rapid Chloride Penetrability (RCP) Test, which is based on the ASTM C1202 [48] and AASHTO T-227 [50] standards. The test was formed after the concrete was allowed to set for 28 days in wet conditions and then allowed to dry in air for one day. Table 5.4.2 specifies the various ranges for Chloride Ion Penetrability based on electrical resistivity results and is based on ASTM C1202 [48] and AASHTO T-227 [50]. The results performed on the dry specimen are tabulated in Table 5.4.1**.** The test results revealed that all the samples yielded electrical resistivity more than 17 kΩ.cm, which lies in the 'moderate' chloride ion penetrability range according to Table 5.4.2**.** This means that mortar layers for all mix formulations will provide moderate resistance when exposed to conditions where chloride particles may pose a threat to the steel wire-mesh reinforcement embedded into the mortar layers.

Table 5.4.1: *Electrical Resistivity Test Results*

Electrical Resistivity Results			
Formulation	**Reading 1 (kΩ·cm)**	**Reading 2 (kΩ·cm)**	**Average (kΩ·cm)**
Control Mix	20.31	21.01	20.66
Fly Ash	19.43	19.7	19.57
Marble Powder	17.1	18.2	17.65

Table 5.4.2*: *Comparison of chloride penetrability levels established for standards based on electrical resistivity (AASHTO TP 95) and charge passed (ASTM C1202)

Sr. No.	**Chloride Ion Penetrability**	**AASTHO TP 95 (kΩ·cm)**	**ASTM C1202 (Coulombs)**
1.	High	<12	>4000
2.	Moderate	12 to 21	2000 to 4000
3.	Low	21 to 37	1000 to 2000
4.	Very Low	37 to 254	100 to 1000
5.	Negligible	>254	<100

The test results also reveal the control mix yielded the greatest resistivity again chloride ions, followed by specimen incorporating Fly Ash (FA) and lastly sample incorporating Waste Marble Powder (WMP). The low electrical resistivity for the WMP sample may be due to the increased porosity as a result of adding WMP in sample. Due to the non-pozzolanic nature of WMP, a higher percentage of unreacted calcium hydroxide forms in the microstructure due to water particles accumulating around the WMP sample [58].

The results for FA15 sample and CM are much more comparable. At 15% replacement of cement by Fly Ash, the dilution effect dominates the chemical effect. The pozzolanic reaction between mineral admixture and Calcium Hydroxide (CH) takes places after 28-day age, which is not studied in the scope of this research [58]; hence, the reduction in porosity because of pozzolanic reaction did not manifest at 28-days age, resulting in FA15 sample possessing a similar pore structure to control sample with slightly reduced electrical resistivity.

5.5 Carbonation

Carbonation was determined using visual inspection by spraying phenolphthalein alcoholic solution onto the exposed surface of the sample. The samples were left in open air for natural carbonation and were tested for signs of carbonation two months after the samples had been set for 28-days. Figure 5.5.1 (a), (b), (c) shows the exposed surface of samples after spraying them with phenolphthalein alcoholic solution. The sprayed samples were tested under a microscope to observe for any signs of carbonation visible on the exposed surface of the sample. Majority of the sample displayed a pink to purplish color suggesting that the pH of the sample if above 8.6 and negligible carbonation has taken place. The exposed cross-section and the slight depth of the sample which remains colorless suggests that carbonation has taken place and the pH of that portion of the sample is below 8.6, suggesting signs of carbonation in the sample [68]

The resulting carbonation depth was found out to be 0.22 mm after two months of exposure in natural conditions. Carbonation rate results is typically indicated in units of $mm/yr^{0.5}$. This is because carbonation if approximately proportional to square root of time [68]. The carbonation rate can be calculated by dividing the depth of carbonation by the square root of time which is two months. This equation results in carbonation

rate of 0.54 mm/yr$^{0.5}$ which means carbonation depth will be 0.54 mm after one year of exposure in natural air, 1.08 mm after four years of exposure in natural air, 1.62 mm after three years exposure in natural air etc. Since a cover of 15mm is provided for the steel wire reinforcement, a simple calculation reveals that it will take 750+ years for carbonation depth to reach the steel wire-mesh reinforcement, making the mortar samples suitable for resistance against carbonation in mild conditions.

Figure 5.5.1: *(a) Specimen Before Testing (b) Surface Carbonation (c) Specimen Split andcheck for carbonation*

Table 5.5.1: *Carbonation rate of Mortar exposed to Natural Carbonation*

Exposure	Time (Days)	Average Carbonation Depth (mm)	Standard Deviation (SD)	Carbonation Rate (mm/yr$^{0.5}$)
Natural Carbonation	60	0.22	0.08	0.54

5.6 Sandwich Panel Test Results and Discussion

5.6.1 Weight and Density

Three scaled wall panels were casted for testing in compression and one scaled slab panel was casted to be tested in flexure. The weight of each specimen after 28-days of wet curing and one-day of dry air curing was obtained using calibrated weight-scales to get the strength/weight ratio for each specimen. The scaled wall panels were 180mm in thickness, 762mm in depth and 305mm in width. The volume of a single wall panel was found out to be 0.042 m^3. The weights and densities of the wall panels are tabulated in Table 5.6.1**.** The average density of the three wall-samples was found out to be 860 kg/m^3. This is significantly less when compared to density of typical construction materials.

The density of R.C.C element is typically between 2400-2500 kg/m^3 and that of structural brick is 1500-1800 kg/m^3. Hence, a lightweight insulated panel is around 2-3 times as light as conventional building materials and is more comparable to special lightweight building materials such as autoclaved aerated concrete blocks, concrete-eps wall panels, lightweight aggregate concrete and hollow brick blocks etc.

***Table 5.6.1**: Weight and Densities of Wall Panels*

Sample	Weight (kg)	Volume (m^3)	Density
Wall Panel 1	36.25	0.042	863
Wall Panel 2	35.45	0.042	844
Wall Panel 3	36.63	0.042	872

5.6.2 Thermal Transmittance (U-Value)

The thermal transmittance (U-value) was found using the Heat Flow Apparatus in USPCAS-E, NUST. The test was performed on scaled wall samples and the results for the thermal resistance (R-value) and thermal transmittance (U-Value) are tabulated in Table 5.6.2**.** The tabulated results represent the average thermal transmittance values at three various temperatures in the temperate ranges of 0-50◦C, which is a representationof the maximum and minimum temperatures in Pakistan.

The average thermal transmittance values for the three samples are within close ranges to each other with a difference of ± 1% between the values. The reason for this minute difference is because the insulation proprieties are primarily due to the EPS insulation layer in between. The average thermal conductivity of a concrete sample is typically 1.5–2.7 W/(m.K.) [69] and that of EPS insulation is 0.0313 W/(m.K.) [70]; hence, since the thicknesses of the concrete layers are equivalent to each other, the resulting thermal conductivity of the three wall samples will almost also be the same.

***Table 5.6.2**: Thermal Conductivity Test Results*

Formulation	Thermal Resistance R-Value (m^{2}K/W)	U-Value for a 180mm Thick Panel (W/m^{2}K)
Control Mix	0.3380	0.389
Fly Ash	0.3422	0.385
Marble Powder	0.3426	0.384

The thermal transmittance values of sandwich panels can also be compared to thermal transmittance values of walls and floors in typical residential construction in Pakistan as specified in Table 5.6.3. The values of traditional construction elements are extracted from [71] and [72]. The thickness of the roof layer for conventional roof slab is almost 18" and that of conventional wall is 8.5", including the additional external insulation provided. As a contrast, the thickness of the sandwich panel floor and wall is 7.5", whichwill result in increases room spaces in structures. The U-value for sandwich floor panelsis almost 3 times lesser compared to conventional roof slabs and 5-6 times lesser than conventional brick masonry and R.C.C walls in residential homes, solidifying the thermal efficiency provided because of incorporating insulation layer.

Table 5.6.3: *Thermal Conductivity Values for a typical building in Pakistan*

Building Component	**Sandwich Structure (W/m^2K)**	**R.C.C Structure (W/m^2K)**	**Brick Masonry Structure**
Roof	0.385	1.020	1.020
Walls	0.385	1.800	2.01

5.6.3 Compressive Strength

The specimens were casted with mortar layer incorporating control mix recipe and the dimensions of scaled wall panels were 760mm x 300mm x 180mm. The specimens were caped for uniform load distribution at the cross-section of the panel. The specimens were tested in compression until maximum load was achieved, where the first macro crack was formed and after which a decrease in load withstood was seen. The compressive strength results are tabulated in Table 5.6.4. The average compressive strength of the three specimen is found out to be 10.73 MPa and the average failure load of the specimens is found out be 609 kN. Trung Bui et al. tested 15 MPa brick masonry walls in compression to test the ultimate strength at bond failure. The brick masonry wall was 150 mm thick, 2000 mm in height and 4000 mm wide. The ultimate load resisted by the brick wall was 630 kN [73]. The compressive strength of the subsequent wall comes out to be 8.2 MPa. Results of the scaled sandwich wall panels display around 23% higher compressive strength and 50% reduction in weight when compared to brick masonry wall construction.

***Table 5.6.4*:** *Compression Test Results for Scaled Panels*

Tests	Density (kg/m^3)	Failure Load (kN)	Compressive Strength (MPa)
Panel 1	863	608.4	10.724
Panel 2	844	615.2	10.840
Panel 3	872	603.4	10.640

During the compression testing of the specimens, cracking was observed running parallel to the lateral surface of the bond between the mortar wythe and the EPS insulation layer. This suggests that the 90-degree shear connectors don't provide adequate shear resistance to resist the shear forces. With the increase in the total compressive load, the width of the crack increased slowly, leading to the failure of specimen as shown in Figure 5.6.1 (a), (b) and (c).

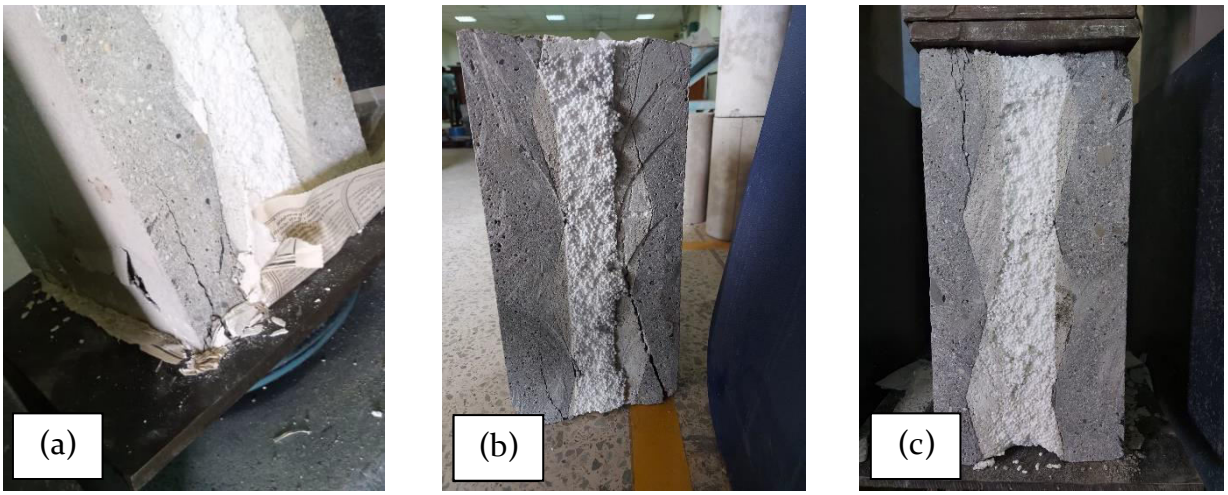

Figure 5.6.1: *(a), (b), (c): Panel failed in compression. Cracks can be seen running parallel to the bond between the mortar and the insulation layer*

5.6.4 Flexure Strength

Flexure strength was found out using three point bending test on a 1500 mm by 1200 mm concrete sandwich slab panel. The specimen was loaded in flexure until the first crack developed at the bottom mortar wythe and a decrease in load was observed. The maximum load withstood at the first crack was found out to be 31.8 MPa. The displacement at first crack was found out to be 5.6 mm.

CHAPTER 6: ANALYSIS OF RESULTS

6.1 Autodesk® Ecotect® Thermal Analysis Results

From the results of the thermal conductivity test for the Lightweight Sandwich Panels, the value of thermal transmittance is found out to be 0.390 W/m²K. While constructing a building envelope for this case, it has been assumed that the roof and wall of the building envelope are made using Concrete Sandwich Panels (CSP), whereas the floors, windows and doors are made from the conventional materials. The summary of the transmittance values (U-values) of building components for all three cases is presented in Table 6.1.1

Table 6.1.1*: *Transmittance Values of Building Components for the three cases

No.	Building Components	Conventional U Value (W/m^2k)	Light weight Panel U Value (W/m^2k)	Masonry Wall U Value (W/m^2k)
1.	Roof	1.020	0.390	1.020
2.	Walls	1.800	0.390	2.00
3.	Doors	2.980	2.980	2.980
4.	Windows	5.430	5.430	5.430
5.	Floor	1.330	1.330	1.330

The results which give us the idea that how much power will be used to maintain the internal thermal condition of the building. Though the results can differ from the real situations, we can make a standard comparison between the building models made from different materials. Figure 6.1.1 shows a visual representation of the internal building temperatures for structure made from Concrete Sandwich Panels, for the temperature ranges 14 degree centigrade to 54 degrees centigrade, after thermal comfort analysis has been carried out. From this figure, we can deduce that the internal temperatures are mostly kept at the cooler side, with slight increase in temperatures observed near windows and doors.

In addition to the visual representation, ECOTECT software also gives a summary of the cooling loads required to main the specified internal temperatures of 25°C. The results of the annual cooling loads for the three cases are given in Table 6.1.2 and from these results, we can conclude that replacing the walls and roofs of conventional buildings

with concrete sandwich panels reduces cooling loads by up to 47.83%. The total units of electricity in kWh consumed by conventional structure are 2163 kWh and that of concrete sandwich panel structure is 1124.45 kWh. Moreover, the mean cost of electricity per unit kWh of electricity consumed in residential buildings is 17.98 PKR (for less than 300 units consumed at off-peak hours) [100]; hence, multiplying this mean cost/kWh by annual units consumed reveals cost savings more than 18,500 PKR annually in cooling loads for a small 740 ft² single-story residential home.

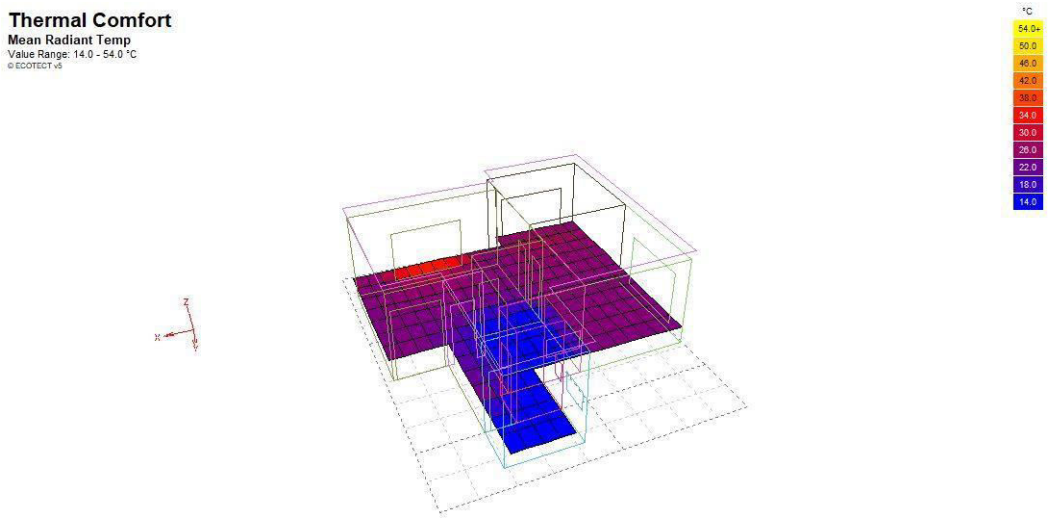

Figure 6.1.1: *Energy Model in Autodesk ECOTECT*

Table 6.1.2*: ECOTECT Thermal Analysis Cooling Load Results*

Building Type	**Annual Cooling Loads (kWh)**	**Annual Cooling Load Cost (R.S)**	**Annual Reduction in Cooling Loads**
Light Weight Panel	1124.45	20217.611	-
Brick Masonry Structure	2163.502	38899.766	47.83%
Concrete Block Structure	2117.617	38074.754	46.7%

Figure 6.1.2: *ECOTECT Analysis Results showing annual cooling loads in kWh*

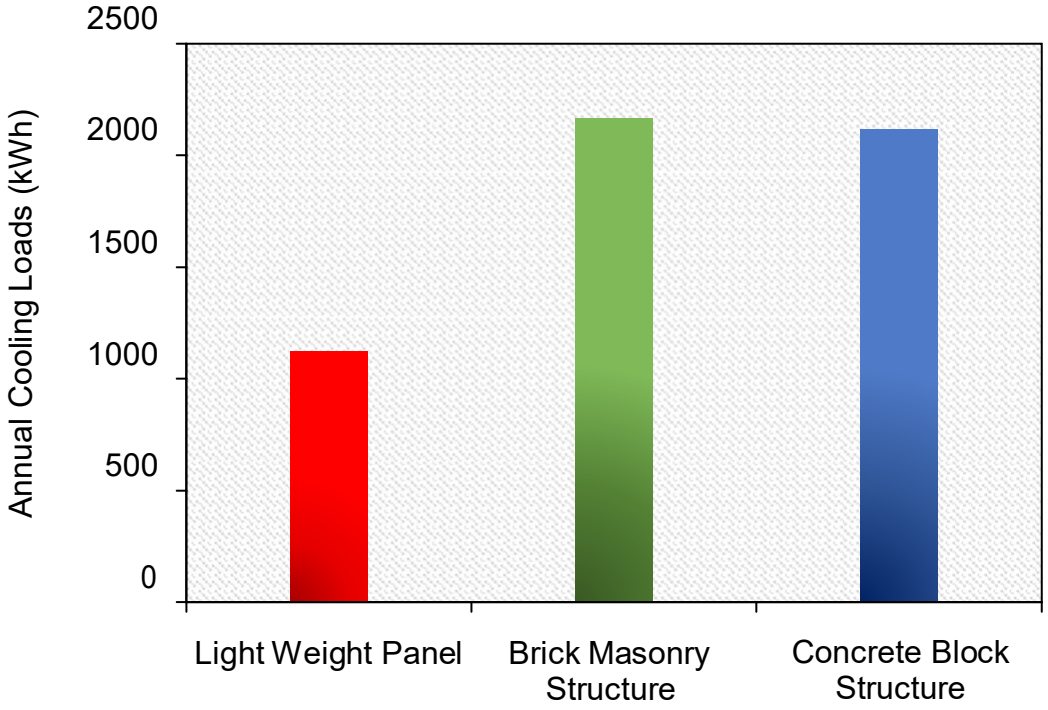

6.2 Carbon Footprint

6.2.1 Manufacturing Stage

The proposed panels are manufactured in a size of 1.2m in width and 3m in height using 50±2mm thick cement mortar skin on either side. The overall thickness of panel is 186 mm. The embodied energy of an individual panel was evaluated by considering the materials used for one batch. The approximate individual materials used per one panel are given in Table 6.2.1**.** Similarly, for the sake of comparison, walls with equivalent dimensions made of concrete and brick masonry were considered and their respective embodied energy during the manufacturing stage was calculated to serve as a basis for comparison. The calculated for material quantities for single panels are given as follows:

- Volume of mortar per panel = 1.2 x 3.05 x 0.10 = 0.366 m^3
- Mass of cement per panel = (0.85/4.1) x 2200 x 0.366 = 167 k
- Mass of Fly ash per panel = (0.15/4.1) x 2200 x 0.366 = 167 kg
- Volume of EPS Foam per panel = 1.2 x 3.05 x 0.08 = 0.2928 m^3
- Mass of EPS Foam per panel = 15 kg/m^3 x 0.2928 m^3 = 4.39 kg
- Mass of plasticizer = 1% by weight of binder = (167+29.45) x 1% = 1.9645 kg

Table 6.2.1: *Embodied Energy Calculations for One Sandwich Panel*

Material	Quantity (kg)	Energy Intensity	Embodied Energy
		kg CO_2/kg	**kg CO_2**
Cement	167	0.912	152.3
Fly Ash	29.45	0.004	0.12
Sand	609.05	0.006	3.65
Plasticizers	1.9645	1.88	3.69
EPS Foam	4.39	2.5	10.975
Steel Wire Mesh	16.7	0.269	3.23
Total Embodied Energy of Material Used per panel			**174 kg-CO_2**

Similar to the material quantity calculations for lightweight panels, calculations for bricks and concrete in equivalent dimensioned of 1.2m by 3m wall were carried out and tabulated in Tables 6.2.2 and Table 6.2.3.

Table 6.2.2: *Embodied Energy Calculations for 10' x 4' concrete wall*

Concrete Mix (25 MPa)	Quantity (kg)	Energy Intensity	Embodied Energy
		kg CO_2/kg	**kg CO_2**
Cement	340	0.912	310.10
Sand	850	0.004	3.40
Aggregate	850	0.00747	6.35
Total Embodied Energy of Material Used per panel			**320 kg-CO_2**

Table 6.2.3: *Embodied Energy Calculations for 10' x 4' brick wall*

Brick Masonry	**Number of Bricks in Equivalent Volume**	**Energy Intensity**	**Embodied Energy**
		kg CO_2/unit	**kg CO_2**
Bricks	320	5.502	1760.64
Lime Mortar	143 kg	0.891	127.413
Total Embodied Energy of Material Used per panel			**2355.5 kg-CO_2**

The results of carbon emissions at manufacturing stage show that 174 kg of CO_2 is expelled while manufacturing one panel, whereas building a concrete panel with similar dimensions results in carbon emissions of 320 kg, which is roughly an 83.9% increase when compared to lightweight panels. Moreover, burning a single clay brick emits 5.502 kg of CO_2 while manufacturing and with a 1.2 m x 3 m wall of 9" thickness requiring 320 bricks to construct, in addition to 143 kg of lime mortar, a similar dimensioned wall panel made of bricks exerts 2355.5 kg of carbon dioxide during its manufacturing. This number is roughly equivalent to 12.5 times the carbon dioxide emitted while constructing a concrete sandwich panel.

Table 6.2.4: *Summary of Carbon Emissions for the Three Cases*

Building Type	**Embodied energy (kg CO_2)**	**Percentage Increase**
Light Weight Panels	174	-
Brick Masonry	320	83.91%
R.C.C	2355.5	1254.7%

6.2.2 CO2 Emissions as a Result of Cooling Load

The results of ECOTECT summarized in Table 6.1.2 gave cooling load values in kWh required to maintain moderate internal temperatures inside home. This value can be multiplied by the average yearly value for carbon emissions from power sector in Pakistan. Yousuf et al., carried out a research for carbon emissions resulting from power production in Pakistan and found out that roughly 0.707 ton of CO_2 is emitted while producing 1 MWh of power [103]. Hence, using simple calculations, we can determine the CO_2 emissions for cooling loads. Moreover, if residential structures in Pakistan have an approximate average life of 40 years, we determine the lifetime carbon emissions because of cooling loads. The results for CO_2 emissions per year and for a 40-year-old building are tabulated in Table 6.2.5. Lightweight concrete sandwich panels emit approximately 30 tons less carbon dioxide when compared to conventional construction technologies

Table 6.2.5: *Carbon Emissions for Building with 40-year Design Life*

Building Type	Cooling load (MWh)	CO_2 Emission/year	CO_2 Emission in 40 years	Reduction
Light Weight Panels	1.124	0.786 ton of CO_2	31.46 ton of CO_2	-
Brick Masonry	2.163	1.530 ton of CO_2	61.2 ton of CO_2	47.8%
R.C.C	2.117	1.497 ton of CO_2	59.88 ton of CO_2	46.5%

6.3 Material Cost Analysis

To determine the financial feasibility of sandwich panels for construction, their material cost is compared to material cost of brick masonry structure and R.C.C structure to construct a single room with the following dimensions:

- Dimensions = 12’ x 12’
- Slab Thickness = 6”
- Wall Thickness = 9”

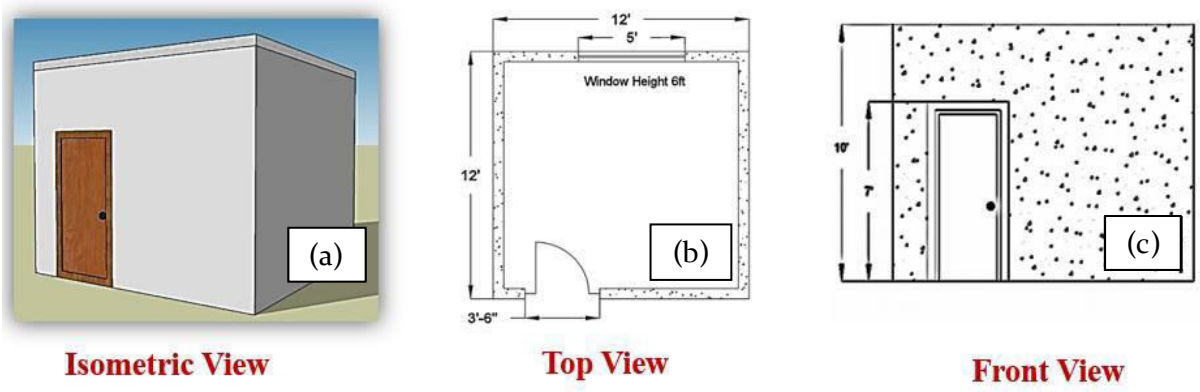

Figure 6.3.1 *: (a) Isometric View (b) Top View (c) Elevation View of a 12' x 12' room*

Table 6.3.1: *12' x 12' Concrete Sandwich Panel Room Material Cost*

Wall Calculations				
Material	**Quantity(ft^3)**	**Bags**	**Rate**	**Cost**
Cement	157.44	-		
Sand	38.4	31	645	19814.40
EPS	119.04	-	35	4166.40
Wire mesh	92.5	-	162.5	15031.25
Panel Roof	480	-	130	62400.00
Slab Calculations				
Cement	47.232			
Sand	11.52	9	645	5944.32
EPS	35.712		35	1249.92
Wire mesh	45		162.5	7312.50
Flooring	144		150	21600.00
Flooring Calculations				
Badal Grey Marble	144		46	6624.00
Cement	72			
Sand	10.30	8	645	5307.40
Aggregate Sargodha	20.60		35	720.00
Rori	41.14		65	2674.30
Water Proofing	180		27.5	4950.00
Footing	180		75	13500.00
	2.4		2	1290.00
Total Cost				173988

Table 6.3.2: *12 ' x 12 ' Brick Masonry Room Material Cost*

Wall Calculations				
Material	**Quantity(ft³)**	**Bags**	**Rate**	**Cost**
Number of Bricks	4860		12	58320.00
Mortar	2592			31104.00
Cement	4.50	4	645	2580.00
Sand	28.49		35	997.32
Plaster (1:6)	15.74			
Slab Calculations				
Grade 60 Steel	204		138	28152.00
Concrete (1:2:4)	72			
Cement	10.30	9	645	5805.00
Sand	20.60		35	720.00
Crush	41.14		80	3291.43
Flooring Calculations				
Badal grey marble	144		46	6624.00
Flooring	72			
Cement	10.30	8	645	5307.43
Sand	20.60		35	720.00
Aggregate Sargodha	41.14		65	2674.29
Rori	180		27.5	4950.00
Water Proofing	180		75	13500.00
Total Cost				164746

Table 6.3.3: *12 ' x 12 ' Brick Masonry Room Material Cost*

Wall Calculations				
Material	**Quantity(ft³)**	**Bags**	**Rate**	**Cost**
Column	27			
Colum Steel	100		138	13800.00
Cement	3.86	4	645	5160.00
Sand	20.60		35	1440.00
Crush	41.14		80	6582.86
Beam	150		138	20700.00

Table 6.3.3 Continued…				
Slab Calculations				
Grade 60 Steel	204		148	30192.00
Concrete (1:2:4)	72			
Cement	10.30	9	645	5805.00
Sand	20.60		35	720.00
Crush	41.14		80	3291.43
Footing	20		138	2760.00
Flooring Calculations				
Badal grey marble	144		46	6624.00
Flooring	72			
Cement	10.30	8	645	5307.43
Sand	20.60		35	720.00
Aggregate Sargodha	41.14		65	2674.30
Rori	180		27.5	4950.00
Water Proofing	180		75	13500.00
Total Cost				182137.40

Table 6.3.4: *Summary of Material Cost for the Three Cases*

Type of Construction	Cost (Rs.)	% Difference
Light Weight Panel	173988	-
Brick Masonry Structure	64745	5.3% cheaper
R.C.C frame structure	182137	4.7% expensive

The summary of the cost analysis is tabulated in Table 6.3.4 and results shows that the material cost for lightweight panels is within ± 5% range to conventional construction materials, making concrete sandwich panels an excellent alternative to conventional building technologies, without significant increase in cost.

CHAPTER 7: CONCLUSIONS AND RECOMMENDATIONS

7.1 Conclusions

1) Sandwich panels comprising of 50 mm mortar wythes and 80 mm EPS insulation layer with steel connectors spaced at 150 mm is adequate in sustaining the expected design load of 27.9 kN evaluated through ASCE 7-16
2) Mortar Wythe recipe is optimized on use of Marble Powder and Fly Ash as indigenous waste at the controlled dose of 15%, ensuring 28-days compressive strength of over 25 MPa.
3) The experiment validates the numerical model on ABAQUS for fabricated sandwich panel in uniaxial compression, offering resistance more than 600kN, making them adequate as structural walls for residential homes.
4) The devised panel reduces cooling loads, operational phase carbon emissions and electricity costs on average by 46% in comparison to brick masonry and R.C.C structures. Further embodied energy released in manufacturing phase releases 13 times less carbon emissions than brick masonry and 2 times less than R.C.C
5) The sandwich panel offers cost-effective solution for rapid and sustainable housing to the low-income societies in Pakistan.

7.2 Recommendations

1) Seismic Analysis of Sandwich Structure
2) Assessing the acoustic performance of lightweight wall panels and comparison with conventional building technologies
3) Testing the full-scale panel in compression and comparing results with a section of the wall to understand and account for effects of de-stabilizing forces and failure
4) Testing sandwich structure for Fire Rating

REFERENCES

[1] http://www.fgeha.gov.pk/noticeboard/prime-ministers-initiative-for-5-million-affordable-low-cost-housing-eoi-rfp/ [CrossRef]

[2] Mahdy M, Imam M, Tahwia A, Yousef O (2010) Study on heat transfer of sandwich panels. In: 7th international engineering conference. Faculty of Engineering, Mansoura University, Egypt [CrossRef]

[3] Mahdy M, Imam M, Tahwia A, Yousef O (2011) Experimental study of structural sandwich members. Housing Build Natl Res J (HBRC) 7(3):48–58 [CrossRef]

[4] Benayoune A, Samad AAA, Trikha DN, Ali AAA, Ellinna SHM (2008) Flexural behaviour of pre-cast concrete sandwich composite panel—experimental and theoretical investigations. Constr Build Mater 22:580–592. [CrossRef]

[5] Daniel Ronald Joseph J, Prabakar J, Alagusundaramoorthy P (2018) Flexural behavior of precast concrete sandwich panels under diferent loading conditions such as punching and bending. Alexandria Eng J 57:309–320. [CrossRef]

[6] Fajrin J, Zhuge Y, Wang H, Bullen F (2017) Experimental and theoretical defections of hybrid composite sandwich panel under four-point bending load. Civil Eng Dimens 19:29–35. [CrossRef]

[7] Daniel Ronald Joseph J, Prabakar J, Alagusundaramoorthy P (2017) Precast concrete sandwich one-way slabs under flexural loading. Eng Struct 138:447–457. [CrossRef]

[8] Amran YHM, Rashid RSM, Hejazi F, Safee NA, Ali AAA (2016) Response of precast foamed concrete sandwich panels to fexural loading. J Build Eng 7:143–158. [CrossRef]

[9] hoi I, Kim JH, You YC (2016) Efect of cyclic loading on composite behavior of insulated concrete sandwich wall panels with GFRP shear connectors. Compos Part B Eng 96:7–19. [CrossRef]

[10] Hosseinpour E, Baharom S, Badaruzzaman WHW, Shariati M, Jalali A (2018) Direct shear behavior of concrete filled hollow steel tube shear connector for slim-floor steel beams. Steel Compos Struct 26:485–499. [CrossRef]

[11] Khorramian K, Maleki S, Shariati M, Jalali A, Tahir MM (2017) Numerical analysis of tilted angle shear connectors in steelconcrete composite systems. Steel Compos Struct 23:67–85. [CrossRef]

[12] Jalali A, Toghroli A, Shariati M, Ibrahim Z (2017) Assessment of stifened angle shear connector under monotonic and fully reversed cyclic loading, pp 64–68. [CrossRef]

[13] Toghroli A, Mohammadhassani M, Suhatril M, Shariati M, Ibrahim Z (2014) Prediction of shear capacity of channel shear connectors using the ANFIS model. Steel Compos Struct 17:623–639. [CrossRef]

[14] Lee JH, Kang SH, Ha YJ, Hong SG (2018) Structural behavior of durable composite sandwich panels with high performance expanded polystyrene concrete. Int J Concr Struct Mater 12:21. [CrossRef]

[15] Tomlinson D, Fam A (2015) Flexural behavior of precast concrete sandwich wall panels with basalt FRP and steel reinforcement. PCI J 60:51–71. [CrossRef]

[16] Kandil, Mohamed & Mahdy, Mohamed & Raheem, Ahmed & Tahwia, Ahmed. (2020). Effect of shear connectors on strength of structural sandwich panels. SN Applied Sciences. 2. 10.1007/s42452-020-03754-3 [CrossRef]

[17] Carbonari, G.; Cavalaro, S. H. P.; Cansario, M.; Aguado, A.: "Flexural behaviour of light-weight sandwich panels composed by concrete and EPS". Constr. Build. Mater. (2012), 35, 792-799. [CrossRef]

[18] Einea, P. E. A.; Salmon, D. C.; Fogarasi, G. J.; Culp, T. D.; Tadros, M. K.: "State-of-the-art of precast concrete sandwich panels". PCI J. November-December 1991, (1991), 78-98 [CrossRef]

[19] Papanicolaou, C. G.; Triantafillou, T. C.: "Minimum cost design of concrete sandwich panels made of HPC faces and PAC core: the case of in-plane loading". Structural Concrete (Journal of the fib). 5, 1, (2002), 11-27 [CrossRef]

[20] Reis, E. M.; Rizkalla, S. H.: "Material characteristics of 3-D FRP sandwich panels". Constr. Build. Mat. 22, 6, (2008), 1009-1018. doi: IO. 101 6/j.conbuildmat.2007.03.023 [CrossRef]

[21] Bush, T. D.; Stine, G. L.: "Flexural behavior of composite precast concrete sandwich panels with continuous truss elements". PCI J. March-April, (1994), 112-121 [CrossRef]

[22] Attard, M. M.; Hunt, G. W.: "Sandwich column buckling – A hyperelastic formulation". Int. J. Solid. Struct. 45, 21, (2008a), 5540-5555 [CrossRef]

[23] Attard, M. M.; Hunt, G. W.: "Column buckling with shear deformations—A hyperelastic formulation". Int. J. Solid. Struct. 45, 14-15, (2008b), 4322-4339 [CrossRef]

[24] Pokharel, N.; Mahendran, M.: “Experimental investigation and design of sandwich panels subject to local buckling effects”. J. Constr. Steel. Res.. 59, 12, (2003), 1533-1552 [CrossRef]

[25] Pokharel, N.; Mahendran, M.: “Finite element analysis and design of sandwich panels subject to local buckling effects”. Thin-Walled Struc.t. 42, 4, (2004), 589-611 [CrossRef]

[26] Mousa, M. A.; Uddin, N.: “Global buckling of composite structural insulated wall panels”. Mater. Des.. 32, 2, (2011), 766-772 [CrossRef]

[27] Aguado, Antonio & Carbonari, G. & Cavalaro, Sergio & Cansario, M.. (2013). Experimental and analytical study about the compressive behavior of eps sandwich panels. Materiales de Construcción. Vol. 63. pp.: 393-402. 10.3989/mc.2013.01812. [CrossRef]

[28] ASTM C150/C150M-20, Standard Specification for Portland Cement. In ASTM Volume 04.01 Cement; Lime; Gypsum; ASTM International: West Conshohocken, PA, USA, 1999; pp. 1–9. ISBN 5919881100 [CrossRef]

[29] ASTM C618-19, Standard Specification for Coal Fly Ash and Raw or Calcined Natural Pozzolan for Use in Concrete. In ASTM Volume 04.02 Concrete and Aggregates; ASTM International: West Conshohocken, PA, USA, 2019; p. 5. ISBN 0-8031-3871-7 [CrossRef]

[30] https://www.cement.org/docs/default-source/fc_concrete_technology/is548-optimizing-the-use-of-fly-ash-concrete.pdf [CrossRef]

[31] http://www.flyash.info/2017/026-fox-woca2017p.pdf [CrossRef]

[32] Ostrowski, Krzysztof & Sadowski, Lukasz & Mellas, Mekki & Toubal Seghir, Nadhir & Żak, Andrzej & Królicka, Aleksandra. (2019). The Utilization of Waste Marble Dust as a Cement Replacement in Air-Cured Mortar. Sustainability. 11. 10.3390/su11082215 [CrossRef]

[33] ASTM C270-14a. Standard specification for mortar for unit masonry. In Annual Book of ASTM Standards 4; ASTM Standards: West Conshohocken, PA, USA, 2003. [CrossRef]

[34] ASTM C494/C494M-08a Standard Specification for Chemical Admixtures for Concrete. In ASTM Volume 04.02 Concrete and Aggregates; ASTM International: West Conshohocken, PA, USA, 2014; pp. 1–10 [CrossRef]

[35] https://www.une.org/encuentra-tu-norma/busca-tu-norma/norma?c=N0058253 [CrossRef]

[36] ASTM. Standard test method for sieve analysis of fine aggregates, C 136–01. In: Bailey SJ, Baldini NC, McElrone EK, Peters KA, Rosiak JL, Simms ST,

Terruso DA, Whealen EA, editors. Annual Book of ASTM Standards Concrete and Aggregates, 2004; vol. 4. No. 4.02. p. 84–8 [CrossRef]

[37] ASTM. Specifications for concrete aggregates, C 33-03. In: Bailey SJ, Baldini NC, McElrone EK, Peters KA, Rosiak JL, Simms ST, Terruso DA, Whealen EA, editors. Annual Book of ASTM Standards Concrete and Aggregates, 2004; vol. 4. No. 4.02. p. 10–20. [CrossRef]

[38] ASTM Standard C305. Standard practice for mechanical mixing of hydraulic cement pastes and mortars of plastic consistency. In ASTM Volume 04.01 Cement; Lime; Gypsum; ASTM International: West Conshohocken, PA, USA, 2014; pp. 18–20 [CrossRef]

[39] ASTM C511-19 Standard Specification for Mixing Rooms, Moist Cabinets, Moist Rooms, and Water Storage Tanks Used in the Testing of Hydraulic Cements and Concretes. In ASTM Standard Guide; ASTM International: West Conshohocken, PA, USA, 2015; pp. 23–25. [CrossRef]

[40] ASTM C192 / C192M-19, Standard Practice for Making and Curing Concrete Test Specimens in the Laboratory, ASTM International, West Conshohocken, PA, 2019 [CrossRef]

[41] ASTM C230 / C230M-21, Standard Specification for Flow Table for Use in Tests of Hydraulic Cement, ASTM International, West Conshohocken, PA, 2021 [CrossRef]

[42] ASTM C1437-20, Standard Test Method for Flow of Hydraulic Cement Mortar, ASTM International, West Conshohocken, PA, 2020 [CrossRef]

[43] ASTM C348-20 Standard Test Method for Flexural Strength of Hydraulic-Cement Mortars. In ASTM Volume 04.01 Cement; Lime; Gypsum; ASTM International: West Conshohocken, PA, USA, 2015; pp. 1–6. 64 [CrossRef]

[44] ASTM C349-18 Standard Test Method for Compressive Strength of Hydraulic-Cement Mortars (Using Portions of Prisms Broken in Flexure). In ASTM Volume 04.01 Cement; Lime; Gypsum; ASTM International: West Conshohocken, PA, USA, 2015; pp. 1–4 [CrossRef]

[45] Shama Parveen, ... Raul Fangueiro, in Sustainable and Nonconventional Construction Materials using Inorganic Bonded Fiber Composites, 2017 [CrossRef]

[46] ASTM C596-18, Standard Test Method for Drying Shrinkage of Mortar Containing Hydraulic Cement, ASTM International, West Conshohocken, PA, 2018 [CrossRef]

[47] Bao Lu, ... Tung-Chai Ling, in Carbon Dioxide Sequestration in Cementitious Construction Materials, 2018 [CrossRef]

[48] ASTM C1202-19, Standard Test Method for Electrical Indication of Concrete's Ability to Resist Chloride Ion Penetration, ASTM International, West Conshohocken, PA, 2019 [CrossRef]

[49] Layssi, Hamed & Ghods, Pouria & Alizadeh, Aali & Salehi, Mustafa. (2015). Electrical Resistivity of Concrete. Concrete International. 37. 41-46. [CrossRef]

[50] AASHTO T 227, 2002 Edition, 2002 - Standard Method of Test for Density, Relative Density (Specific Gravity), or API Gravity of Crude Petroleum and Liquid Petroleum Products by Hydrometer Method [CrossRef]

[51] Jana, Dipayan & Erlin, B.. (2007). Carbonation as an indicator of crack age. Concr Int. 61-64 [CrossRef]

[52] Chen, Ying & Liu, Peng & Yu, Zhiwu. (2018). Effects of Environmental Factors on Concrete Carbonation Depth and Compressive Strength. Materials. 11. 2167. 10.3390/ma11112167. [CrossRef]

[53] ASTM C518-17, Standard Test Method for Steady-State Thermal Transmission Properties by Means of the Heat Flow Meter Apparatus, ASTM International, West Conshohocken, PA, 2017 [CrossRef]

[54] ASTM E1530-99, Standard Test Method for Evaluating the Resistance to Thermal Transmission of Thin Specimens of Materials by the Guarded Heat Flow Meter Technique, ASTM International, West Conshohocken, PA, 1999 [CrossRef]

[55] http://3dbuildtech.co.za/what-is-the-tech/ [CrossRef]

[56] Felekoğlu, Burak & Türkel, Selçuk & Kalyoncu, Hasan. (2009). Optimization of fineness to maximize the strength activity of high-calcium ground fly ash – Portland cement composites. Construction and Building Materials - CONSTR BUILD MATER. 23. 2053-2061. 10.1016/j.conbuildmat.2008.08.024 [CrossRef]

[57] Wang, Xiao-Yong. (2014). Effect of fly ash on properties evolution of cement-based materials. Construction and Building Materials. 69. 32–40. 10.1016/j.conbuildmat.2014.07.029. [CrossRef]

[58] Kondraivendhan, Ba & Bhattacharjee, Bishwajit. (2015). Flow behavior and strength for fly ash blended cement paste and mortar. International Journal of Sustainable Built Environment. 14. 10.1016/j.ijsbe.2015.09.001. [CrossRef]

[59] Ostrowski, Krzysztof & Sadowski, Lukasz & Mellas, Mekki & Toubal Seghir, Nadhir & Żak, Andrzej & Królicka, Aleksandra. (2019). The Utilization of Waste Marble Dust as a Cement Replacement in Air-Cured Mortar. Sustainability. 11. 10.3390/su11082215. [CrossRef]

[60] Vardhan, K.; Siddique, R.; Goyal, S. Strength, permeation and micro-structural characteristics of concrete incorporating waste marble. Constr. Build. Mater. 2019, 203, 45–55. [CrossRef]

[61] Khyaliya, R.K.; Kabeer, K.I.S.A.; Vyas, A.K. Evaluation of strength and durability of lean mortar mixes containing marble waste. Constr. Build. Mater. 2017, 147, 598–607. [CrossRef]

[62] Ashish, D.K.; Verma, S.K.; Kumar, R.; Sharma, N. Properties of concrete incorporating sand and cement with waste marble powder. Adv. Concr. Construct. 2016, 4, 145–160. [CrossRef]

[63] Arel, H. ¸S. Recyclability of waste marble in concrete production. J. Clean. Prod. 2016, 131, 179–188. [CrossRef]

[64] Geso ˘glu, M.; Güneyisi, E.; Kocabag, M.E.; Bayram, V.; Mermerda¸s, K. Fresh and hardened characteristics of self compacting concretes made with combined use of marble powder, limestone filler, and fly ash. Constr. Build. Mater. 2012, 37, 160–170. [CrossRef]

[65] ASTM C157 / C157M-17, Standard Test Method for Length Change of Hardened Hydraulic-Cement Mortar and Concrete, ASTM International, West Conshohocken, PA, 2017 [CrossRef]

[66] AS 3972-2010 General purpose and blended cements [CrossRef]

[67] Moghaddam, A. & Sirivivatnanon, Vute & Vessalas, Kirk. (2019). The effect of fly ash fineness on heat of hydration, microstructure, flow and compressive strength of blended cement pastes. Case Studies in Construction Materials. 10. e00218. 10.1016/j.cscm.2019.e00218. [CrossRef]

[68] https://www.understanding-cement.com/carbonation.html [CrossRef]

[69] Shafigh, P.; Asadi, I.; Akhiani, A.R.; Mahyuddin, N.B.; Hashemi, M. (2020) Thermal properties of cement mortar with different mix proportions. Mater. Construcc. 70 [339], e224 [CrossRef]

[70] Shi, Jinyan & Liu, Yuanchun & Liu, Baoju & Han, Dan. (2019). Temperature Effect on the Thermal Conductivity of Expanded Polystyrene Foamed Concrete: Experimental Investigation and Model Correction. Advances in Materials Science and Engineering. 2019. 1-9. 10.1155/2019/8292379. [CrossRef]

[71] Shaheen, Nafeesa & Arif, Sabahat & Khan, Arif. (2016). Thermal Performance of Typical Residential Building in Karachi with Different Materials for Construction. [CrossRef]

[72] “Thermal Performance of Building Envelope Details for Mid- and High-Rise Buildings (1365-RP),” American Society of Heating, Refrigerating and Air-Conditioning Engineers, Inc. (ASHRAE), Atlanta, GA, 2011. [CrossRef]

[73] Bui, Trung & Limam, Ali & Sarhosis, Vasilis. (2019). Failure analysis of masonry wall panels subjected to in-plane and out-of-plane loading using the discrete element method. European Journal of Environmental and Civil Engineering. 25. 10.1080/19648189.2018.1552897. [CrossRef]

[74] A. Marsh. Ecotect and EnergyPlus Build. Energy Simulat. User News, 24 (6) (2003), pp. 2-3 [CrossRef]

[75] D.B. Crawley, J.W. Hand, M. Kummert, B.T. Griffith. Contrasting the capabilities of building energy performance simulation programs Build. Environ., 43 (4) (2008), pp. 661-673 [CrossRef]

[76] A.H. Abdullah, S.K.A. Bakar, I.A. Rahman. Simulation of office's operative temperature using Ecotect model, Int. J. Const. Tech. Mgt., 1 (1) (2013), pp. 33-37 [CrossRef]

[77] D.I. Ibarra, C.F. Reinhart. Daylight factor simulations–how close do simulation beginners ‘really’ get? Build. Simulat. (2009), pp. 196-203 [CrossRef]

[78] P.R. Vangimalla, S.J. Olbina, R.R. Issa, J. Hinze. Validation of Autodesk Ecotect™ accuracy for thermal and daylighting simulations, Simulation Conference (WSC). Proceedings of the 2011 Winter, IEEE (2011), pp. 3383-3394 [CrossRef]

[79] E. Wang, Z. Shen, C. Barryman. A building LCA case study using Autodesk Ecotect and BIM model, 47th ASC Annual International Conference Proceedings (2011) [CrossRef]

[80] K. Adalberth. Energy use during the life cycles of buildings: a method, Build. Environ., 32 (4) (1997), pp. 317-320 [CrossRef]

[81] G.A. Blengini, T. Di Carlo. Energy-saving policies and low-energy residential buildings: an LCA case study to support decision makers in Piedmont (Italy), Int. J. Life Cycle Assess., 15 (7) (2010), pp. 652-665 [CrossRef]

[82] M.K. Dixit, C.H. Culp, J.L. Fernández-Solís. System boundary for embodied energy in buildings: a conceptual model for definition, Renew. Sust. Energy Rev., 21 (2013), pp. 153-164 [CrossRef]

[83] T. Ramesh, R. Prakash, K.K. Shukla. Life cycle energy analysis of buildings: an overview, Energy Build., 42 (10) (2010), pp. 1592-1600 [CrossRef]

[84] M. Suzuki, T. Oka. Estimation of life cycle energy consumption and CO2 emission of office buildings in Japan, Energy Build., 28 (1) (1998), pp. 33-41 [CrossRef]

[85] Y.G. Yohanis, B. Norton. Including embodied energy considerations at the conceptual stage of building design, Proc. Inst. of Mech. Eng. A J. Power Energy, 220 (3) (2006), pp. 271-288 [CrossRef]

[86] Arif, S., Khan, A., and Alamgir, K., "Modeling the Temperature Effect of Orientations in Residential Buildings", Mehran University Research Journal of Engineering & Technology, Volume 31, No. 3, pp. 371-378, Jamshoro, Pakistan, 2012. [CrossRef]

[87] https://www.dawn.com/news/1520402 [CrossRef]

[88] Cheung, C.K., Fuller, R.J. and Luther, M.B., "EnergyEfficient Envelope Design for High-Rise Apartments", Energy and Buildings, Volume 37, No. 1, pp. 37-48, January, 2005. [CrossRef]

[89] Arif, S., Khan, A., Mushtaq, M., and Alamgir, K., "Orientation and House Plan Configuration For Energy", Pakistan Journal of Science, Pakistan Association for Advancement of Sceince, Volume 65, No. 2, pp. 292-295, Lahore, Pakistan, 2013. [CrossRef]

[90] Arif, S., Khan, A., and Alamgir, K., "Environmental Issues and Energy Conservation in Buildings in Pakistan: Role of Architectural Intervention", Nucleus, Volume 2, No. 2, pp. 137-142, Isalmabad, Pakistan, 2011. [CrossRef]

[91] Tang, R., and Etzion, Y., "On Thermal Performance of an Improved Roof Pond for Cooling Buildings", Building and Environment, Volume 39, No. 2, pp. 201-209, February, 2004. [CrossRef]

[92] Ahmed, K., Arif, S., Khan, A., and Mushtaq, M., "Effect of Low Cost Roof Insulating Materials on Indoor", Pakistan Journal of Science, Pakistan Association for Advancement of Sceince, Volume 65, No. 2, pp. 239-242, Lahore, Pakistan, 2013. [CrossRef]

[93] Balaras, C.A., "The Role of Thermal Mass on the Cooling Load of Buildings. An Overview of Computational Methods," Energy and Building, Volume 24, No. 1, pp. 1-10, January, 1996. [CrossRef]

[94] Strong, K.S., "Sustainable Urban Neighborhoods", Thesis of M.Arch, University of Florida, Florida, 2001. [CrossRef]

[95] Khan, A., Arif, S., and Alamgir, K., "Thermal Loads Agaianst Building Orientation for Susutaianable Housing in Pakistan", Mehran University Research

Journal of Engineering & Technology, Volume 31, No. 3, pp. 371-378, Jamshoro, Pakistan, July, 2012. [CrossRef]

[96] Bahrami, S., "Energy Efficient Buildings in Warm Climates of the Middle East," Masters Thesis, Lund, Swidon, October, 2008. [CrossRef]

[97] Gut, P., and Ackernecht, D., "Climatic Responsive BuildingAppropiate Building Construcvtion in Tropical and Subtropical", Niedermann AG, St. Gallen , 1st Edition, Skat, Switzerland,1993. [CrossRef]

[98] Wong, N.H., and Li, S., "A Study of the Effectiveness of Passive Climate Control in Naturally Ventilated Residential Buildings in Singapore," Building Environment, Volume 42, No. 3, pp. 1395-1405, March, 2007. [CrossRef]

[99] http://www.karachi.climatemps.com/ [CrossRef]

[100] https://www.ke.com.pk/assets/uploads/2021/02/Consumer-Schedule-of-Tariff.pdf [CrossRef]

[101] Peng, C. (2016). Calculation of a Building's Life Cycle Carbon Emissions Based on Eco-tect and Building Information Modeling. Journal of Cleaner Production, 112, 453-465. [CrossRef]

[102] Yang, X., Hu, M., Wu, J., & Zhao, B. (2018). Building-Information-Modeling Enabled Life Cycle Assessment, a Case Study on Carbon Footprint Accounting for a Residential Building in China. Journal of Cleaner Production, 183, 729-743. [CrossRef]

[103] I. Yousuf, A.R. Ghumman, H.N. Hashmi, M.A. Kamal, "Carbon emissions from power sector in Pakistan and opportunities to mitigate those, Renewable and Sustainable Energy Reviews", Volume 34, 2014 [CrossRef]

[104] G.Rasul et al. 2012b. Climate Change in Pakistan Focused on Sindh Province. Technical Report. No. 25. Islamabad: Pakistan Metrological Department [CrossRef]